Chapter 4

Fibonacci Nanostructures for Novel Nanotherapeutical Approach

Lidija Matija*, Jelena Muncan*, Ivana Mileusnic*, Djuro Koruga*,**

**University of Belgrade, Belgrade, Serbia; **European Center for Peace and Development (ECPD), United Nations-Mandated University for Peace, Belgrade, Serbia*

Chapter Outline

1 INTRODUCTION

Through human history, people always tried to improve their everyday lives, to make it easier for living and to prevent diseases. To achieve these goals, human beings were watching nature and trying to understand its laws. For example, one of the oldest human wishes was to fly, and through research and watching the birds, aircraft was invented. In the same manner, by biomimicry, in any part of our lives we were following nature and its rules, especially in science. Humans are following the natural rules not only in science, but in art, too. It is well known that mankind admire Egypt's pyramids and the Greek's temples. The question is why they are so special, and the answer is simple—they were built according to beauty and sublime principle, known as the Golden Mean law. This law is the essential one for human beings because our DNA is following that law. This is because the mathematical law controlling by self-organizing of the basis T, C, A, G inside of DNA was discovered (Perez, 2015; Rakočević, 1998). It was found out (Perez, 2013) that the consecutive sets of DNA nucleotides are organized in frames of the distant order called "RESONANCES." Here "Resonance" represents the special proportion ensuring division of DNA parts pursuant to the Fibonacci numbers that lead us to Golden Mean law. In addition, it was reported that this law is the driving force of protein biomolecular machinery (Koruga, 1997).

Bearing in mind that Fibonacci law (the Golden Mean), as a driving force of biomolecular machinery, it is very important to know how internal structure (DNA proteins and water) reacted on the external random stimuli. However, to date, the scientific efforts to process the external influence on biomolecular machinery is still not well known. Biological structures on molecular levels are unique entities where mass, energy, and information are in a synergy state. The main function of DNA is presented as protein coding. Until 2013 our knowledge related to DNA signaling was based on the biochemical

Nano- and Microscale Drug Delivery Systems. http://dx.doi.org/10.1016/B978-0-323-52727-9.00004-2

donor–acceptor approach. Twelve years ago nonprotein (amino acids)-coding sequences, called a "junk" one, are identified as functionally coding sequences of DNA. Gene activity, based on traditional view, is changed, on exon active sequences for protein coding and on intron noncoding protein sequences (amino acids). In the process of mapping from DNA to RNA the intronic and the exonic are separated in messenger RNA. There is no purpose during mapping information from RNA to protein. A new view of gene activities gives a more complex explanation of DNA, RNA, and protein mapping than a complicated one (Mattick, 2003).

One of the important issues is how to improve the efficiency of the external stimuli action. A promising approach is to start from classical (bulk) substance to micro and nanosubstance. For example, if length of one size of 3D box substance is 20 μm for pharmaceutical treatment, as external stimuli, then the total surface area for interaction is 2400 μm^2. However, if some volume of substance having the length of one size of substance is 2 μm then the total surface area for interaction is 24,000 μm^2. In this case efficiency is 10 times higher, while efficiency of stimuli can increase more than 1000 times if nanomaterials are used. Nanoapproach is not only a challenge for external stimuli efficiency but also to establish personal nanomedicine, as a goal to overcome the limit of classical medicine, which is now more statistical. In addition, it is important to make innovation inspired by nature—to make nanostructures for synergetic external/internal stimuli based on biomimicry. Regenerative medicine offered a solution—bone engineering concept that mimics cell differentiation process of embryogenesis. In cases of serious, massive damages of the bones, in order to save extremities, synthetic bone is created. In the bioengineering process, cells are planted on a three-dimensional scaffold in vitro, and exposed, in vitro or in vivo, to the environment full of osteogenic, angiogenic, and mechanic embryonic nanosignals.

Similar to autologous graft, four factors are necessary: (1) three-dimensional scaffold as a conductive element, (2) stem cells, which produce new tissue, (3) bioactive inductive cell signals, which control and lead, in time and space, cell differentiation processes, and production of a new bone tissue, (4) nutritional (nourishing) factor, and good vascularization are very important for sufficient blood supply. A critical component in this process that mimics natural healing of bone tissue is scaffold. In order to play a role of base on which new bone tissue will be formed, it should fulfill several conditions, such as: (1) nanointerconnected porosity, (2) surface of nanopores should be appropriately prepared to ensure cell growth and proliferation and transport of nutriments and by-products, (3) anticipative resorption and remodeling by products not threatening to osteogenic activity, (4) release of cell biosignals for cell differentiation controlled in time and space, (5) mechanical properties similar to bone tissue and stable relation material/tissue during healing process, (6) immunologic compatibility without rejecting potential, (7) good adaptation of surrounding tissue.

The discovery of fullerene C_{60} and a whole family of a spherical molecular crystal form of carbon, bound by single and double bonds, creating three-dimensional, Fibonacci nanostructures, fullerenes, in 1985 (Kroto et al., 1985) brought the revolution in the science and opened a new field—nanotechnology. Soon after, the discoveries of carbon nanotubes (CNTs) in 1991 (Iijima, 1991) and graphene in 2004 (Novoselov et al., 2004), carbon-based nanomaterials have attracted numerous researchers in different fields of science to work on their application, due to their excellent properties generated by its structure and fivefold symmetry, which are also ruled by Golden Mean (Koruga, 1993). Icosahedral symmetry of structure determines new mechanical, optical, and electrical properties unknown before (Feng and Liu, 2011; Geim, 2009; Sanchez et al., 2011), and they found a great deal of interest in various biomedical applications (Cha et al., 2013; Lee et al., 2012), such as gene delivery (Bao et al., 2011), optical imaging (Li et al., 2012), and nanotherapeutics (Li et al., 2012; Ngan et al., 2015; Wang et al., 2008; Yang et al., 2012, 2014; Yin et al., 2013, 2014; Zuo et al., 2013).

These various applications of carbon-based nanomaterials also increased concern related to their interactions with tissues, cells, and biomolecules (Nel et al., 2009), influence on the integrity of cells (Nel et al., 2006; Zhao et al., 2008) as well as their impact on structure and function of proteins and nucleic acids (Ge et al., 2011; Kang et al., 2012b). A deep understanding of the interaction between nanomaterial and biomolecules, at the molecular level is a key for the proper and safe design and application of nanoparticle-based biomedical technologies (Chen et al., 2006; Donaldson et al., 2006; Gilbert, 2009; Nel et al., 2006; Service, 2000; Zhang et al., 2010; Zhao et al., 2008; Zuo et al., 2013).

Many experimental and theoretical studies on the interactions among proteins, nucleic acids (such as DNA), and cell membranes with the zero-dimensional (0D) fullerenes, one-dimensional (1D) carbon nanotubes (CNTs), and two-dimensional (2D) graphene have demonstrated a serious cytotoxicity and biosafety concerns because these interactions can affect both the structures and functions of biological systems (Kang et al., 2012a; Lanone et al., 2013; Zhang et al., 2014; Zuo et al., 2013).

Here we are proposing a biophysical nano approach, behind which Golden Mean law is: how nanomaterials may influence DNA (from extracellular space trough cell membrane to nucleus) in order to help repair damaged structure by their biophysical influence.

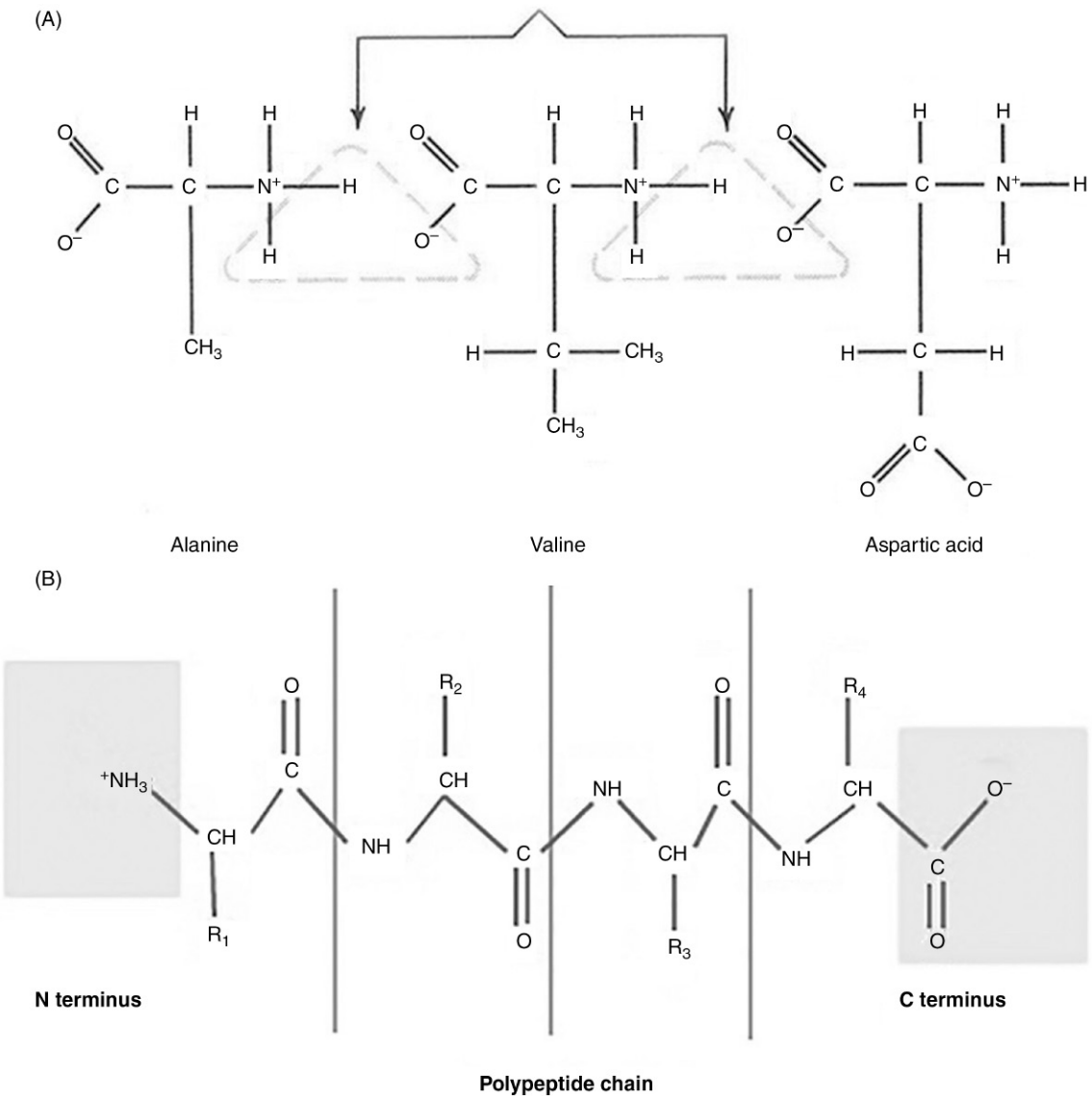

FIGURE 4.1 (A) Polypeptide chain formation from amino acids giving two molecules water per a peptide plane. (B) This new structure giving new properties to system, polypeptide chain is more biophysical than biochemical entity.

2 MOTIVATION

Biological systems are nanosystems because DNA in chromosome, as a major coding macromolecule of biological body, is 2 nm in diameter and about 1.5 m long. It has been shown that DNA structure is determined by the Golden Mean law (Perez, 2013; Rakočević, 1998). The ternary DNA code system ($4^3 = 64$) is primary one for assembling amino acids in a protein chain and is a code of structural order that has a limited role for protein functionality. Since binary DNA code ($2^6 = 64$) has same number of 64 code words as ternary code; it is bridge between classical (ternary) and quantum state of protein chain (Rakočević, 1998). The force constant of hydrogen bonds between two DNA bases (A═T, GC) has an average value of 80 N/m, with both classical (Colombo law) and quantum (Schrödinger law) properties. It is well known that the force constant in a peptide plain is several times smaller than in nonorganic matter (C—C: 434 N/m in a peptide plane, C—C: 2500 N/m in diamond). From an information point of view binary code of DNA ($2^6 = 64$) opens the possibility to investigate proteins as quantum information devices ($2^{n+1}-1$), the "second side of DNA code." In our investigation both classical (Lagrangian) and quantum (Hamiltonian) approaches have been used to characterize peptide plains (Koruga, 2012). On the other hand, bearing in mind that both DNA and fullerenes, especially C_{60}, are following the Golden Mean law, it is

possible to make nanomaterials that will help in treating diseases or preventing them. This is also because they proved to be very effective in biomedical applications.

DNA acts in two ways, chemically and physically, and in two modes, classical and quantum (Koruga, 2012). The mechanism of action is very complex and only partially known. In part of biomolecular signaling we are giving evidence of DNA-protein-water signaling, which is related to healthy/unhealthy state of tissues. In addition to the motivation to understand the mechanism of signal transduction at the biomolecular level, we considered it our special challenge to create the material/device that will act by this mechanism. To this end, we have designed Fibonacci nanostructures and tested it (case study) for wounds, burns, and skin cancer.

3 BIOMOLECULAR SIGNALING AND FIBONACCI NANOSTRUCTURES

3.1 Biomolecular Signaling

The ability of cells to sense and react to their surroundings governs their capacity to proliferate, develop, differentiate, and maintain tissue homeostasis. Deficiencies in appropriately translating environmental cues underlie many forms of cancer, neurodegeneration, and immune dysfunction. The critical signaling that occurs in response to external stimuli is often initiated at the surface of cells and traverses a network of membrane bound compartments, to ultimately elicit changes in cellular gene expression and metabolism. How these signaling pathways are effectively integrated to facilitate a defined cellular response is a major focus of membrane biology and cell signaling science.

3.2 Fibonacci Nanostructures in Biology: Classical and Quantum Approach

As they appear everywhere in nature people believe that nature's numbering system is based on Fibonacci numbers. Fibonacci sequences are everywhere: as pattern form in plants, ratio of dimensions (length) in antic monuments (Parthenon), ratio of surface in old Egypt monuments like pyramids, and so on. Processes describing the growth of every living thing, from single cell to all of mankind, are determined by the Fibonacci numbers.

For example, Fibonacci number law is present in embryogenesis, the cochlea of the inner spiral ear forms, and as ratio of the forearm and the hand. Also, the best works of art have been created by Fibonacci laws as a process of the artist mind mapping on canvas.

The Fibonacci numbers are seen in the proportions in the sections of a finger, too.

These are only few examples of macroscopic evidence of Fibonacci structures in biology. However, hidden to our eyes, on a molecular level like DNA, microtubules, collagen, and other biomolecules, the Fibonacci law also occurs (Koruga, 1993; Rakočević, 1998).

To investigate presence of Fibonacci law of numbers on molecular and nanolevels it is necessary to consider both classical and quantum properties. An illustrative example is peptide plane and its chain in proteins (Fig. 4.1A–B).

The basic criteria to determine whether the peptide plane possesses classical or quantum mechanical property is calculation of action of each atom. If action value, as product of energy and time, is close enough to Planck constant, than process of object, or field process, can be considered as quantum mechanical entity. It is well known that Planck constant h has property of action with value 6.626×10^{-34} J s. To understand process it is necessary to define limit value of atomic action in peptide plane that will not violate its quantum mechanical properties. Planck constant is a bridge between both particles and wave, and energy and oscillation. To solve dilemma classical or quantum properties of entity electrical and magnetic interactions between two electron charges in neighboring atoms in relative motion in the peptide plane has to be investigated. To calculate the magnetic interaction between two charged particles in motion relative to an observer O by Coulomb's law is very difficult. If the process is simplified then it is possible not to calculate exact value of the magnetic and electrical interactions, but to compare its orders of magnitude. To do it, it is necessary to consider two charges q and q' of neighboring atoms moving at velocities $\boldsymbol{v}$ and $\boldsymbol{v}'$ relative to the observer. The electrical force produced by q' on q, measured by O, is qE. The magnetic field (B) produced by q' may be calculated as:

$$B = \frac{1}{c^2}(vE) \tag{4.1}$$

Since the order of magnitude of B is given by $v'E/c^2$, then the magnetic force on q, as ratio of v, v', and c is:

$$qvB = \left(\frac{vv'}{c^2}\right)qE \tag{4.2}$$

Bearing in mind that qE is the electrical force on q, then the ratio of *magnetic force/electrical force* is (F_M/F_E) is determined by vv'/c^2 order value. In many cases, when the velocities of the charges are small compared to the velocity of light c, the magnetic force can be ignored. Since the orbital velocity of valence electrons in atoms is approximately around $\sim 10^6$ m/s, then vv'/c^2 gives ratio $F_M/F_E \times 10^{-4}$. Order of four, between electrical and magnetic forces of valence electrons, gives that both classical and quantum phenomena simultaneously exist in range $10^{-34} < h^* < 10^{-30}$ J s. For any value higher than 10^{-30} J s phenomena are pure classical, while if it is less than 10^{-34} J s, it is pure quantum.

Planck constant h is composed of force, 1D space, and time and may be represented as product of $\boldsymbol{F}$ (force), $\boldsymbol{d}$ (displacement from equilibrium state), and $\boldsymbol{t}$ (time of action) (Koruga, 2012):

$$h = A = F \times d \times t \ (\mathrm{J\,s}) \tag{4.3}$$

The force (F) can be calculated as a product of a force constant k_f and bond length x between any two coupling atoms in the peptide plane as:

$$F = k_f d \times x \tag{4.4}$$

Known bond lengths (x_i) are: C—C = 132 pm, C—N = 145 pm, C—O = 124 pm, NH = 102 pm. According to Eq. (4.4), the force between C—C can be calculated as (Koruga, 2012):

$$F_{C-C} = 434 \times 132 \cdot 10^{-12} = 57.28 \cdot 10^{-9}\,\mathrm{N} \tag{4.5}$$

Minimal action (A) between C—C is then:

$$A_{\min}\left(57.28 \cdot 10^{-9}\right) \times \left(25 \cdot 10^{-12}\right) \times 10^{-13} = 1.43 \cdot 10^{-31}\,\mathrm{J\,s} \tag{4.6}$$

While the maximal action is:

$$A_{\max}\left(57.28 \cdot 10^{-9}\right) \times \left(85 \cdot 10^{-12}\right) \times 10^{-13} = 4.86 \cdot 10^{-31}\,\mathrm{J\,s} \tag{4.7}$$

According to Eqs. (4.6) and (4.7) the action value for any two coupling atoms in the peptide plane is smaller than 10^{-30} J s and higher than 10^{-34} J s it can be conclude that the peptide plain from the action (energy × time) point of view is a *quantum-fractional* entity: neither classical nor quantum.

There are many thousands of different types of proteins in living systems but microtubules are the most interesting from classical and quantum physics, which are related to information processing. Microtubules as complex biomolecular systems are a unique synergetic entity of classical mechanics, quantum mechanics, and information. A new scientific paradigm has been born based on microtubules, clathrin, and water clusters, as Fibonacci structures, in biological systems by the Golden Mean law (Koruga et al., 1992).

3.3 Model of Peptide Plane Oscillation

If the ratio of peptide plain and peptide chain is considered as ratio of part/whole, then the Lagrangian model of electron oscillation could be applied (Fig. 4.2). Since working space of action is considered as a charge field then the basic charge of an atom has not only main covalent connection but several other lateral connections In this case beside the main covalent

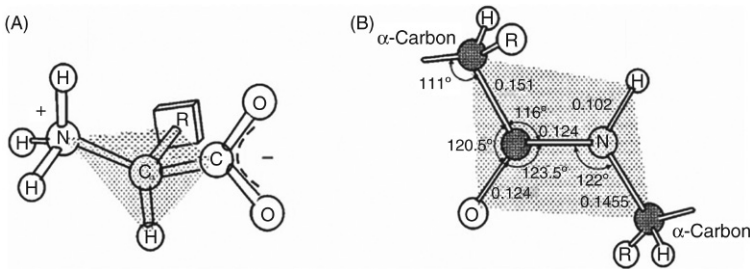

FIGURE 4.2 Amino acids are the basic chemical structure for protein building. They are the other side of the DNA structural-information code. As a tetragonal structure, they have two groups (N and C, known as terminals), group R (different from each type of amino acids), and two atoms Cα and H (A). Atoms in peptide plain are on about 100 pm distances. Peptide plain is composed of half of each two neighboring amino acids in protein chain (B), except only N-terminal as a first half of the first amino acid (usually methionine) and C-terminal at the end of protein chain (Matija and Koruga, 2007).

connection in the working space of action exists lateral connections, which are much weaker. This classical-quantum approach, based on Lagrange equation, is a more natural solution for peptide plain dynamics than using Hamiltonian, which happens because applying Hamiltonian more assumptions have to be taken than applying Lagrangian. If dynamics of peptide plain is considered as usual quantum entity for the vibrational analysis of polyatomic molecular structures, then quantum-mechanical Schrödinger equation with the Born–Oppenheimer perturbation method (Bernstein, 1992) and Frölich-like model is offering a solution but with high numbers of assumptions (Samsonovich et al., 1991). However, using the working action space approach and applying either Lagrange equation $d/dt\,(\partial T/\partial x_j') - \partial T/\partial x_j = Q_j$ or Hamiltonian $ih/2\pi\,(\partial\psi/\partial t) = -H\psi$ on peptide planes oscillatory process in protein chain, the results will be approximately the same.
Here, the dynamics of amino acids are considered in the limited chain, and in state of equilibrium, when the Lagrange equation is equal to zero. Under these conditions potential force is $Q_j = -\partial V/\partial q_j$, and if $\partial T/\partial q_j = 0$ and $\partial V/\partial q_j' = 0$, then the Lagrange equation is:

$$\frac{d}{dt}\left(\frac{\partial T}{\partial x_s'}\right) + \frac{\partial V}{\partial x_s} = 0 \tag{4.8}$$

Using the approach of working action field, it turns that all four forces in biomolecules and cells: gravitational, magnetic thermal, and electrical are in equilibrium. When the Lagrange equation is equal to zero, then the oscillation system can be investigated as an oscillator with reduced mass. For oscillatory dynamics, force constants are used and each entity (atom) of peptide plain oscillate around its equilibrium with displacements in x, y, z directions. Bearing in mind that peptide plain is 2D object oscillation of atoms in peptide plane should be investigated in two dimensions. It means that one direction has to be eliminated, like x_2 ($x_2 = -m_1/m_2(x_1 + x_3)$). Under this condition the kinetic energy (T) in Eq. (4.8), for the two body system with m_1 and m_2, becomes:

$$T = \frac{m_1}{2}\left(1 + \frac{m_1}{m_2}\right)x_1'^{\,2} + \frac{m_1}{2}\left(1 + \frac{m_1}{m_2}\right)x_3'^{\,2} + \frac{m_1}{2}\left(\frac{m_1 2}{m_2}\right)x_1'x_3' \tag{4.9}$$

and the potential energy

$$V = \frac{K}{2}\left\{\left[x_1\left(1 + \left(\frac{m_1}{m_2}\right)\right) + x_3\left(\frac{m_1}{m_2}\right)\right]^2 + \left[\left(x_3\left(1 + \left(\frac{m_1}{m_2}\right)\right) + x_1\left(\frac{m_1}{m_2}\right)\right)\right]^2\right\} \tag{4.10}$$

Distances in 2D space between atoms in peptide plane, are given in Fig. 4.3 (right), while for each atom real connections of corrugate peptide plain are presented in Fig. 4.4.

In action space, for every atom of peptide plain, there are four equivalent atom connections in a mutually orthogonal direction. All six atoms of peptide plain, with its connections, are indirectly included in determination of proper frequency. In total there are 4 connecting and 6 neighboring atoms of peptide plain, which give summary 10 of them. This provides

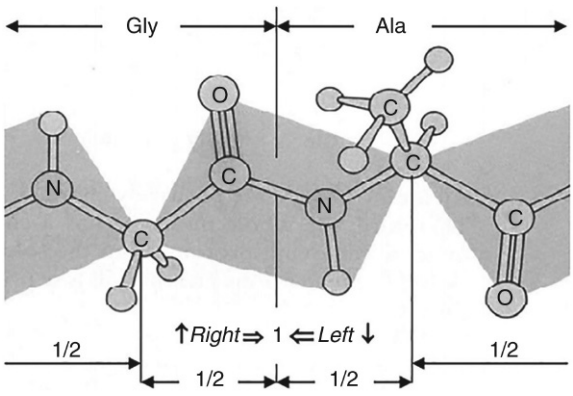

FIGURE 4.3 The protein chain is built by the chemically structural information code of DNA. When established, the protein chain becomes a physical energy-information code capable of transmitting oscillatory information from N- to C-terminal and to group R, which preserves chemical properties of amino acids in protein (Matija and Koruga, 2007).

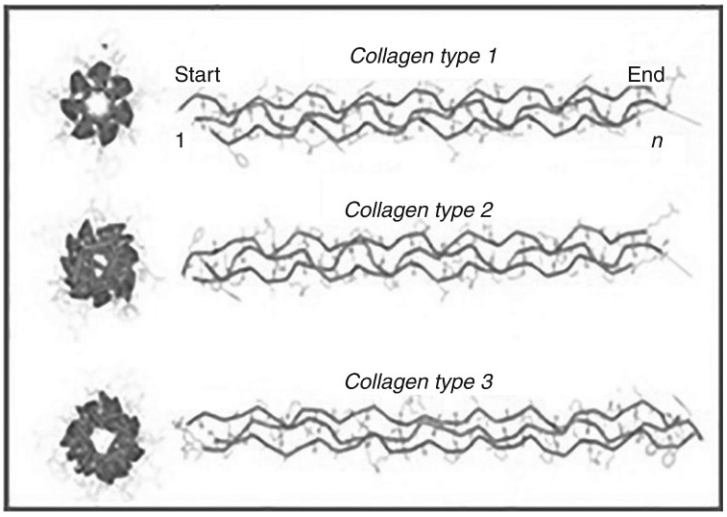

FIGURE 4.4 Oscillation of peptide planes in three types of collagen.

the evidence that vibration of atoms in peptide planes and rotation of peptide planes around C atom with and angles exist. For calculation, force constant K and the value of vibration-rotation energy has to be included.

If an atom in bond is not in proposed directions, as in the proposed model, it means that atoms will be divided in two parts. In this situation the same mass and new coefficients will be determined by actual solution, which will be modified with coefficients of angle. Force constant K, as coefficient of elasticity, can be calculated as:

$$K = 4\pi^2 m\left(\frac{\Delta E}{h^2}\right) \tag{4.11}$$

where m is reduced mass $(m_1 \times m_2)/(m_1 + m_2)$, $\Delta E = h\nu_0$; h is Plank constant and ν_0 is frequency (ν_0 can be taken from Raman and IR spectra). Also, frequency ν_0 can be calculated using ΔE and force constant $K = e^2/4\pi\varepsilon_0 d^3$ [from Eq. (4.11)], where e, value of charge; ε_0, vacuum permittivity; and d, distance between two centers of charge in equilibrium state.

Using Eq. (4.11) values of K are calculated for: C═O it is 1850 N/m; C═C, 1080 N/m; C—C, 434 N/m in $H_3C—CH_3$, while for diamonds C—C is 2500 N/m (Matija and Koruga, 2007). According to experimental results these values are in good agreement with book references (Kuhn and Forsterling, 2000).

Oscillatory frequencies m_G for atom in protein chain with N atoms, with two perpendicular modes, are given by Eq. (4.12).

$$\omega_G^2 = \frac{K_3}{m_G} + \frac{K}{m_G} 4\sin^2\frac{n\pi}{2(N+1)} = \omega_{GY}^2 + \omega_{GX}^2 \tag{4.12}$$

A model of chain oscillator, with N-bond number along basic oscillating channel, gives the possibility for calculation parameters: K-bond coefficient (force constant); m_G and m_R, mass of "head" and of "tail" of amino acid (Koruga, 2012).

Peptide plane consists of two amino acids; forward part of one and backward part of another, and represents planar structure, with some quasiparticle properties. This biophysical property arises because deformed clouds of electrons give additional strength. In addition, the synergetic effect of harmonization of electric force, magnetic force, gravity, and heat of the peptide chain in living matter makes distances between atoms larger than in nonliving matter (Jeffrey, 1997).

Using larger distances between atoms in xy plane of the peptide plain, the oscillations of atoms are calculated. However, peptide plane in protein chain oscillate in −C–N–C–C− chain, direction (x-axis), along its normal (y-axis) and along tail normal to peptide plane (z-axis). Synergetic oscillation of atoms in three planes: xy, yz, zx is presented in Fig. 4.4.

Comparing to classical physics, in general and thermodynamic property, in particular, proteins are nanosystems with a relatively small number of atoms. Since atoms are discrete structures, they are in order by crystallographic symmetry, while their peptide planes and secondary structures are dynamic entities whose energies have smooth changes, close enough to continuum property (Blundell and Johnson, 1976). Using Eqs. (4.5)–(4.12), the oscillation of atoms in peptide plane in all tree directions are calculated; along large diagonal (x-axis), along its normal (y-axis), and along tail normal to peptide plane

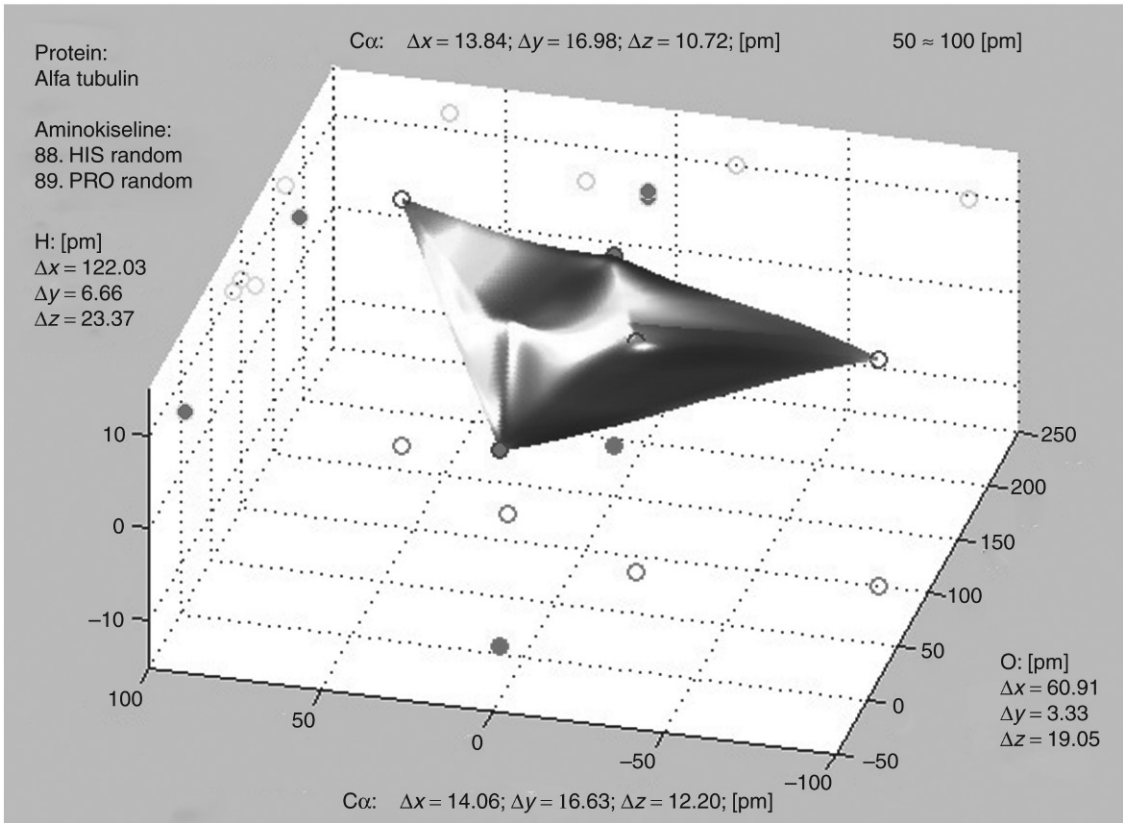

FIGURE 4.5 Peptide plane as a 2D corrugate structure, like "nanobutterfly." In reality peptide plane is 3D quasiparticle because thickness of peptide plain is on level of size of atom. Particular state of peptide plane on this picture is determined by parts of amino acid HIS (*histidine*) at positions 88 and PRO (*proline*) in position 89 in alpha tubulin's random structure (Koruga et al., 2004).

(*z*-axis). For each amino acid in chain, choosing of code number [*N* in Eq. (4.12)] takes in account organizational parts of secondary structure of protein: -helix, -plane, and random array.

Based on the model of peptide planes oscillation presented in this chapter, a program for computer simulation is developed. In Fig. 4.5, one can see how two amino acids, threonine and glycine, formed the peptide plane. Peptide plain is 3D quasicondensate of six atoms. Change is presented from equilibrium point in *x*, *y*, and *z* directions. Value of change (displacement) is in picometer (pm), and set of Δy, Δz values is the parameter of peptide plane deformation from ideal state.

As is known, atoms are quantum mechanical objects, while peptide plane is one of the first biological structures (condensate) with dual properties, quantum and classical mechanical. High resolution measurements by AFM of the mechanical force between microtubule and kinesin motor proteins (tail–tail interaction) is about 5 pN, with the loading rate is less than 1 pN/s (for 20 s→1,8 pN, 25 s→3,7 pN, and 30 s→5,4 pN) (Koruga et al., 2004). According to physical properties between electrical, mechanical, and thermal properties (like piezo and pyro effects) of peptide plane and protein chain coupling effects may exist. For example, macroscopic mechanical forces may produce a piezo effect similar to sparks in our eyes, when we receive a quick mechanical hit to them. It arises from biological crystal structure of molecules (billions of alpha helixes of rhodopsin biomolecules transform mechanical energy into piezoelectric).

Peptide plane is a structure with both crystallographic symmetry group and Curie limit symmetry group (Curie, 1894). Oscillation is nondeterministic chaotic process capable of generating classical and quantum information processing. From that point of view proteins, as coding structure, possess molecular cooperative energy codes, which lead to energy-information code responsible to control protein conformation change (Koruga et al., 2004). For example, there is strong frequency coupling of the set of first three peptide planes and last three in collagen chain is:

$$\Delta v_1/\Delta v_2/\Delta v_3 = \varphi/1,2/1, \tag{4.13}$$

$$\Delta v_{335}/\Delta v_{336}\Delta v_{337} = e/\varphi/1 \tag{4.14}$$

According to Eqs. (4.13) and (4.14), the approach of working action space results in peptide plane oscillations of collagen that are very harmonized. The measure of harmony process, energy of peptide plane to compare with energy of protein chain, is Golden Mean number ϕ (0.6183), while process optimization of energy distribution peptide planes and information process trough peptide chain is done by $e^x = 2.718282$, for unit value $x = 1$ (Koruga et al., 2004). It means that synergy of the energy-information process in biomolecules has to be based on *e,* as statistical biomechanical signaling phenomena.

3.4 Cell–Matrix Interactions

Cell–matrix interactions play an important role in the control of cellular differentiation, morphogenesis, proliferation, and migration, and consequently have also impact on processes, such as embryogenesis, wound healing, inflammation, and cancer. Many of these interactions with the extracellular matrix are interfered with by the integrin family of cell adhesion molecules (Jones and Walker, 1999).

Integrins are a large family of type I transmembrane heterodimeric glycoprotein receptors and are composed of noncovalently associated dissimilar α and β subunits. Integrins exist as two noncovalently bound α and β subunits, which couple to form heterodimers (Jones and Walker, 1999; Srichai and Zent, 2010). To date, 18 α and 8 β known subunits have been described and combine to form at least 24 distinct integrin heterodimers (Hynes, 2002; Srichai and Zent, 2010). Most integrins function as receptors for extracellular matrix (ECM) proteins, but mediate heterotypic cell–cell adhesion. They can bind to extracellular ECM glycoproteins including collagens, fibronectins, laminins, and cellular receptors as well as the intercellular cell adhesion molecule family (Hynes, 2002; Plow et al., 2000; Srichai and Zent, 2010). The particularity of integrin binding to ECM components including laminins, collagens, and fibronectin depends on the extracellular domains of the α and β integrin subunits. Besides their adhesive function, integrins play an important role in the assembly of the actin cytoskeleton as well as in modulating signal transduction pathways that control biological cellular and integrin receptor function can be considered as a key modulator of cellular behavior (Jones and Walker, 1999; Schwartz et al., 1995; Srichai and Zent, 2010).

Integrins can arbitrate signaling by two mechanisms: "inside out" signaling and "outside in" signaling (Juliano and Haskill, 1993; Schwartz et al., 1995). The first one presents inside out signaling the mechanism by which a cell regulates the affinity state of its integrin receptors, while the second one mediates signals from the extracellular matrix after integrin ligation and involves regulation of many fundamental cellular processes (Schwartz et al., 1995). In "inside out" signaling, it is considered that integrins involve the propagation of conformational changes from the cytoplasmic domains to the extracellular binding site in response to intracellular signaling events (Jones and Walker, 1999). In the case of "outside in" signaling, integrins mediate signals from the extracellular matrix after its ligation and involves regulation of many fundamental cellular processes (Jones and Walker, 1999; Schwartz et al., 1995).

Collagen signaling is occurring by oscillatory process of 1000 peptide planes according to Eq. (4.12). It is well known that collagen is composed of three main (glycine, proline, and lysine) and three additional (valine, alanine, and asparagine) amino acids. The very first peptide plane from N-terminal oscillate with $\Delta\omega_1 = 865.06 \times 10^{11}$ s, second one in order with $\Delta\omega_2 = 658.84 \times 10^{11}$ s, while third one with $\Delta\omega_3 = 533.62 \times 10^{11}$ s. The ratio of frequency of three very first peptide plane in collagen protein chain ($\Delta\omega_1/\Delta\omega_2/\Delta\omega_3$) is ϕ/1.20/1, while for very last three it is e/ϕ/1. It means that signaling follows the Fibonacci law (the Golden Mean in notation ϕ).

Collagen secondary structure is composed of 100% of α-helix, while integrin and tubulin, besides α-helix consist of β-sheets and *R*-random structures. Collagen is distributed in extracellular matrix, integrin penetrate cell membrane and tubulin is part of cell cytoplasma.

In Fig. 4.6A is presented as an energy difference between two successive peptide planes in collagen, or energy distribution that is actually nothing else than configurational entropy of the system. One can notice only one very smooth line, which presents peptide planes energy distribution and this is a consequence of collagen secondary structure that is 100% alpha helix. In the case of integrin (Fig. 4.6B) and tubulin (Fig. 4.6C), the energy distribution is different because their secondary structure consists of alpha and beta sheet randomly arranged. Protein chain follows energy law distribution by secondary structure type regardless peptide plane position within its structure. Bearing in mind that peptide planes of same secondary structure form memorize previous one energy value, we can say that aforementioned property is equivalent to memory. Alpha helix energy distribution (top line), beta planes (middle line), and random structure (bottom line) are presented on Fig. 4.6B. By comparing energy distributions between collagen and integrin (alpha helix), we can conclude that they are very similar. This conclusion is reasonable having in mind alpha helix secondary structure that exists in both proteins. It is very interesting that calculation is showing that same energy distribution has random structure in alpha and beta tubulin subunits.

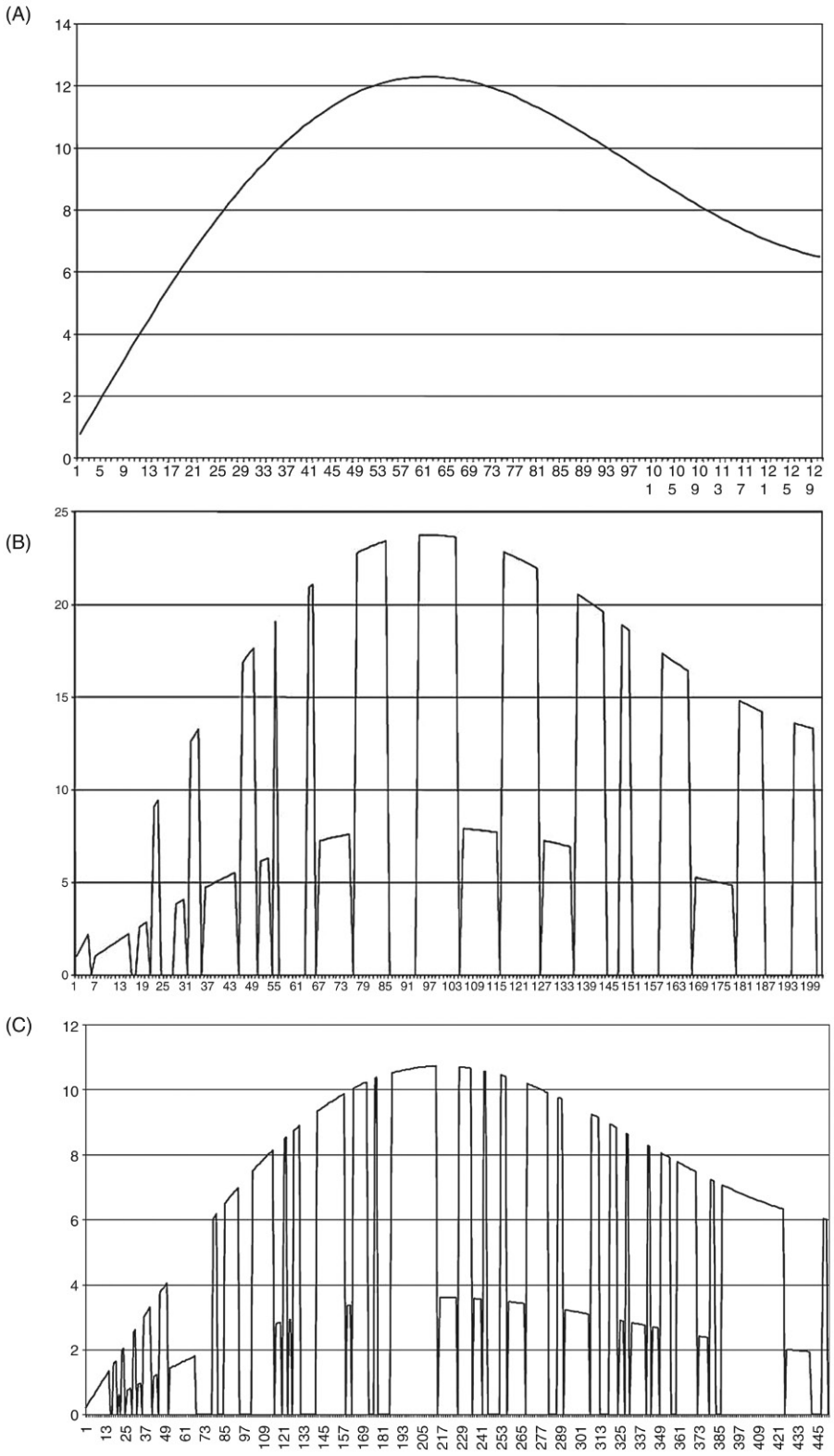

FIGURE 4.6 Diagrams of configurational entropy distribution of collagen (A), integrin (B), and tubulin (C). Ordinate: $\Delta E = E_i - E_{i-1}$, apscise: N_i, position of amino acid in chain (Koruga et al., 2004).

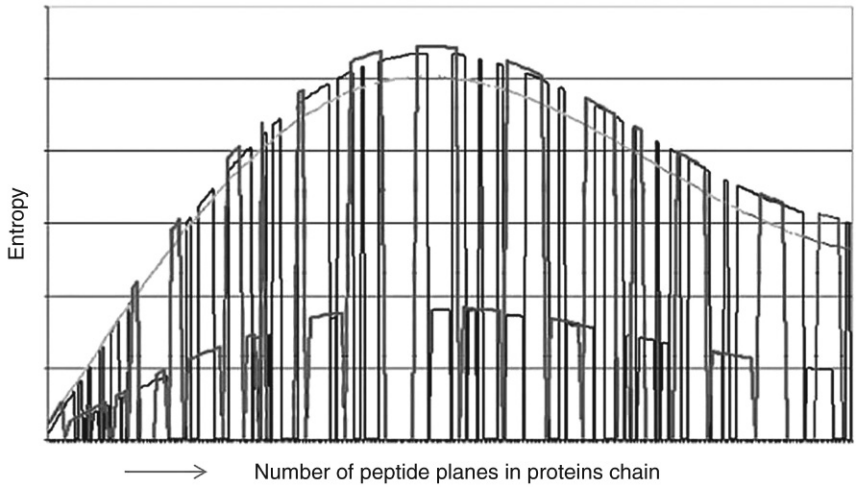

FIGURE 4.7 Summary diagram of collagen-integrin-tubulin energy distribution of peptide planes. Ordinate: $\Delta E = E_i - E_{i-1}$, apscise: N_i, position of amino acid in chain. There is very good overlapping of energy distribution based on peptide plane oscillation (Koruga et al., 2004).

Nevertheless, random structures have a maximal energy level in tubulin subunits (helix has lesser ΔE), while in beta plane it is opposite. A high level of energy distribution consistency in collagen, integrin, and tubulin is presented on Fig. 4.7.

If we apply energy distribution law, we can observe that peptide chain has energies distribution in an assembly of N peptide planes that follows Gibbs statistical mechanics:

$$\frac{N_i}{g_i} = \frac{1}{e^{\alpha + \frac{\Delta E_i}{kT}}} \tag{4.15}$$

where N_i is the energy level population ΔE_i, and g_i is degeneracy (number of possible states with same energy level). The peptide plane is called Gibbson in honor of the outstanding contribution of Josiah Willard Gibbs (1839–1903) in science.

Since Gibbs energy distribution law and the Golden Mean law exist between collagen, integrin, microtubule, and nucleus, then direct the physical link, as well as energy coherence, as main relations schematically is presented in Fig. 4.8. We have discovered that harmony based on the Golden Mean law [Eqs. (4.13) and (4.14)] exists in proteins oscillation of each peptide plane in set of three plains (*as part*), and protein chain (*as whole*). Since amino acid, per se, is a primary biochemical entity in the cell, and peptide plane is consisting of half of each neighboring two amino acids (except *N* and C terminals—beginning and the end of chain), is primary biophysical entity, than protein chain is a new *binary/ternary* entity, in which chemical and physical properties of amino acid are coupled and make synergetic effect. From this approach point of view signal travels through protein chain, as a *binary/ternary* energy-information system of amino acids in peptide planes synergy, then it can be presented as a code:

$$2^0/3^1 + 2^1/3^2 + 2^2/3^3 + 2^3/3^4 + 2^4/3^5 + 2^5/3^6 + 2^6/3^7 + \cdots\cdots + 2^N/3^{N+1} \cdots = 1, \tag{4.16}$$

that is normalized probability distribution (2^0 represents N-terminal and 3^{N+1} represents C-terminal, giving protein chain primary dipole properties).

The irregularity in energy distribution and information disharmony can be induced by irregularities of structural damage (symmetry braking) and conformational change under environmental influence, or wrong bonding (ion–dipole, dipole–dipole), what consequently leads that natural harmony in biological systems, on molecular level, will be endangered. This can happen when alpha helix structures receive energy from collagen trough integrin to tubulin, due to induction of magnetic field and therefore cell energy will be increased and consequently equilibrium violation will occur. In fact, this is the mechanism of how the cell is making self-protection in a case of undesirable extra cellular influences.

Nevertheless, disorder in intracellular communications function is possible to be repaired if the influence by adequate light is induced or by delivering biocompatible nanomaterial in tissue. This is in the case when both light and nanomaterial follow Golden Mean law from an energy point of view. In addition, chosen nanomaterial has to fit between two peptide plains of protein similar to collagen in extra cellular space. This is achievable when torsion angles of nanomaterials (having icosahedral or dodecahedral symmetry) are compatible to the torsion angles φ and ψ of amino acids because nanomaterial will weakly touch peptide plane and transfer its torsion energy. In this case, the link between nanomaterial and protein chain

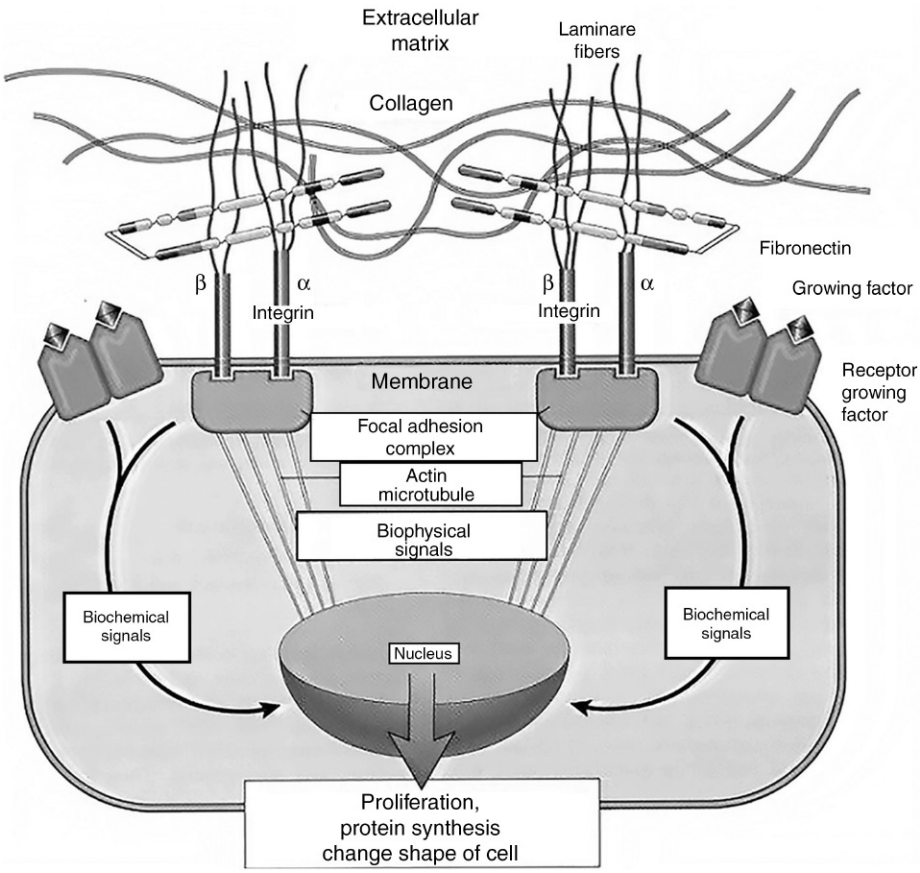

FIGURE 4.8 Model of biophysical communication. Collagen-integrin microtubule nucleus as a feedback system capable for adaptation (Koruga et al., 2004).

will be established by weak interactions, like hydrogen bond, ion–dipole or dipole–dipole interaction and torsion energy. It means that "golden energy states" (T_{1u},T_{2u},T_{1g}, and T_{2g} of HOMO–LUMO) will be transferred into protein chain from the nanomaterial that possess icosahedral symmetry. It will be allowed to nanomaterial energy states, which are following Golden Mean law to travel as an impulse from cell membrane to nucleus through biomolecular network. The explained mechanism will help activation of both cell proliferation and protein syntheses, and therefore nonfunctional cells and proteins will be replaced by new ones. Here, we are presenting, based on the biophysical approach, and describing in vivo experiment using fullerol, molecule with icosahedral symmetry, and Golden Mean property, the first proof of Gibbson application in nanomedicine.

As the Lagrangian model presented earlier offers the possibility for investigation of protein chain oscillation with a few thousand atoms calculation, we used it to calculate frequencies for each atom in chain skeleton or atoms associated to skeleton following peptide planes oscillation. A biophysical coherence, based on the Gibbson approach, between collagen, integrin, and tubulin, having harmony ruled by the Golden Mean law discovered. This indicates that new approaches are possible in order to better understand synchronicity and fast biophysical pathway of communication, which arise between extracellular matrix and cytoplasm as well as between cell membrane and nucleus. A new approach for analyzing biomolecule behavior by influence of external thermal, electromagnetic, and mechanical perturbations is proposed because Lagrangian-based model is applicable to many other biological structures.

4 FIBONACCI NANOSTRUCTURES/C_{60}

Any structure with icosahedral and dodecahedral symmetry is Fibonacci structure. If structure is on nanolevel size, then it is a molecular spherical crystal. One well-known structure is molecule C_{60}. Even more, not only that structure follows Fibonacci law but also energy because it is based on the vibrational mode of atoms lattice of molecular crystal (Table 4.1).

TABLE 4.1 Icosahedral Symmetry Group Which Represents Molecular Crystal C_{60}

I/I_h	E	$12C_5$	$12C_5^2$	$20C_3$	$15C_2$	i	$12S_{10}$	$12S_{10}^3$	$20S_6$	15σ	III	IV	
A_g	1	1	1	1	1	1	1	1	1	1		$x^2+y^2+z^2$	
T_{1g}	3	$1/2(1+\sqrt{5})$	$1/2(1-\sqrt{5})$	0	−1	3	$1/2(1-\sqrt{5})$	$1/2(1+\sqrt{5})$	0	−1	(R_x,R_y,R_z)		
T_{2g}	3	$1/2(1-\sqrt{5})$	$1/2(1+\sqrt{5})$	0	−1	3	$1/2(1+\sqrt{5})$	$1/2(1-\sqrt{5})$	0	−1			
G_g	4	−1	−1	1	0	4	−1	−1	1	0			
H_g	5	0	0	−1	1	5	0	0	−1	1		$(2z^2-x^2-y^2,$ $x^2-y^2,xy,yz,zx)$	
A_u	1	1	1	1	1	−1	−1	−1	−1	−1			
T_{1u}	3	$1/2(1+\sqrt{5})$	$1/2(1-\sqrt{5})$	0	−1	−3	$-1/2(1-\sqrt{5})$	$-1/2(1+\sqrt{5})$	0	1	(x,y,z)		
T_{2u}	3	$1/2(1-\sqrt{5})$	$1/2(1+\sqrt{5})$	0	−1	−3	$-1/2(1+\sqrt{5})$	$-1/2(1-\sqrt{5})$	0	1			$(x^3,y^3,z^3)[x(z^2-y^2),$ $y(z^2-x^2),z(x^2-y^2),xyz]$
G_u	4	−1	−1	1	0	−4	1	1	−1	0			
H_u	5	0	0	−1	1	−5	0	0	1	−1			

Notations A_g, T_{1g}, etc. represents eigenvalue energy of system; E, C_n, S, etc. represent symmetry; while values of $½(1-\sqrt{5})$, etc. represents one of four of the Golden mean state (Koruga, 1993).

Nanomaterials, given their small size, and surface/volume ratio offer many possibilities in manipulating matter on nanoscale, and their potential in the field of health care and cosmetics is well recognized and a subject of worldwide research.

In the field of nanomaterials, fullerenes and their water soluble derivatives, such as fullerols, are shown to be potent radical scavengers, which make this class of nanomaterials attractive tools for regulation of the free radical processes and reducing oxidative stress (Gharbi et al., 2005; Nielsen et al., 2008). It was considered that high antioxidative potential of fullerenes is determined by the ability of C_{60} to bind free radicals (Wang et al., 1999) because with 30 double bonds, it can scavenge up to 60 radicals. However, results obtained by Andrievsky et al. (2009) showed that one hydrated C_{60} is able to neutralize a greater number of hydroxyl radicals than theoretically possible binding capacity of fullerenes is. This observed phenomenon could not be explained by the simple model of radical trapping by fullerene molecules, but instead another mechanism is proposed to explain it. The proposed model emphasizes a key role of mobility–limited superficial water layers and corresponds with the so-called "exclusion zone" water discovered by Pollack et al. (Chai and Pollack, 2010; Zheng et al., 2006). According to this concept, water molecules near hydrophilic surfaces can form long-range stable and ordered water layers, extending to a distance more that 10–100 μm. It is suggested in the study by Andrievsky et al. that hydrated fullerenes being very hydrophilic and highly stable donor–acceptor complex "C_{60}–H_2O molecules" are able to induce in aqueous media the long-range and ordered water shells, which are able to "catalyze" accumulation and deactivation of free radicals. Furthermore, the second probable mechanism of antiradical activity of this fullerene-based water complex, may be in limiting diffusion of free radicals from the loci of their formation, and because of this, immediately after the formation, free radicals are able to recombine fast-yielding molecular products. This way, the fullerene-based water complexes achieve a dual role—they organize the water molecules in stable, long-range water shells, and consequently, due to this organization, antiradical activity is achieved.

The hypothesis is therefore that a hydrated, hydroxylated fullerenes are a class of nanomaterials, which can be used in treating skin in diseases and during aging, and when topically applied in a form of skin cream, they can reorganize part of the water in skin that is not bound to biomolecules. Furthermore, due to this reorganization of water in skin, the formed fullerene-water complexes would also perform a role of antiradical defense system.

In this study, a new type of nanomaterial—hydrated, hydroxylated fullerene is used, which is one form of fullerene derivate—fullerol, around which a water stabilizing belt is created (Fig. 4.9). This new nanomaterial is named nanoharmonized substance (NHS) (Koruga, 2011).

The core of this new nanomaterial is the molecule C_{60}, which generates beneficial vibration by the Golden Mean law (Matija et al., 2012). The importance of Golden Mean law in creating biofunctional nanomaterials was discussed in a previous publication concerning nanoharmonized substance (Matija et al., 2013). The addition of hydroxyl groups (Fig. 4.9) makes fullerene water soluble. A water-stabilizing belt has been made around carbon hydroxyl molecule (Fig. 4.9) in order to overcome issues with fullerene toxicity. It is reported that the addition of hydroxyl groups and nanolayers of water around fullerene makes it nontoxic in concentrations of 10^6–10^9 ppb (Matija et al., 2013). Thus, newly created nanoharmonized substances can be considered safe and potentially beneficial for cosmetic and medical applications. Since its structure is based on Golden Mean law, water-based nanoharmonized substance (wNHS) can present Golden Mean driving force of self-assembly processes in biological tissues and lead to recovery of disrupted biomolecular functions (Matija et al., 2012, 2013).

The proposed hypothetical model of water reorganization of water by NHS nanomaterial is presented in Fig. 4.10. It is based on the Andrievsky et al. model (Andrievsky et al., 2009).

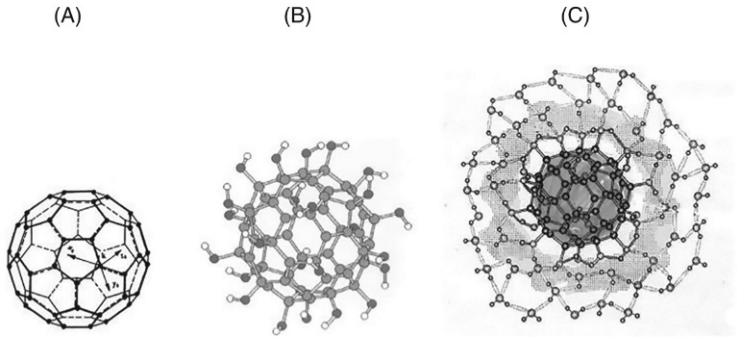

FIGURE 4.9 Three different molecular structures based on Fibonacci nanomaterial. Molecule C_{60} (A), hydrogen bonded $C_{60}(OH)_x$ (B), and energetically stabilized nanoharmonized substance $C_{60}(OH)_x@(H_2O)_y$ (C) (Matija et al., 2012, 2013).

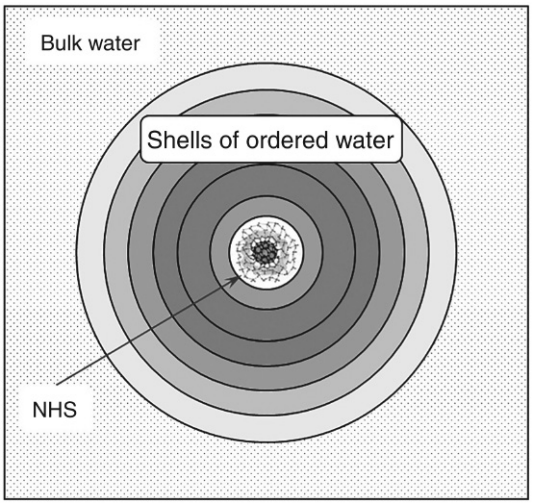

FIGURE 4.10 Proposed model of organizing water around nanoharmonized substance (NHS).

4.1 Water–DNA Hydrogen Bonding

The importance of hydrogen bonding for the structure and consequently the function of biological macromolecules is not a new concept in science. The very concept of hydrogen bond, can be attributed to M.L. Huggins and W.M. Latimir who proposed it in 1919 and 1920, independently from one another, according to one of the greatest pioneers in water science, Linus Pauling. Since most biological organisms contain free water fractions ranging from 60% to 80%, hydrogen bond emerges as very important for the functioning of all important biological molecules.

There are two types of chemical bonds important for water: *hydrogen bonds* between water molecules and *sigma bonds* within a single water molecule forming between oxygen and hydrogen atoms. It is well understood that the nature of covalent bonds may only be described by the laws of quantum mechanics because each electron does not really belong to a single atom—it belongs to both simultaneously. However, for a long period of time, it was believed that hydrogen bond could be perfectly understood by principles of electrostatic interactions described by the Coulomb's law or in the other words, laws of classical physics, based on attraction and repulsion forces existing between charged particles. Only recently, experimental data have shown some indications that hydrogen bond has a dual nature—classical and quantum (Isaacs et al., 1999). These new evidences mark the key point for our understanding of DNA and protein interaction with water. Furthermore, water itself may be a coding structure because due to extensive hydrogen bond networks it can organize in clusters. DNA and microtubules may act as generators of water organized in large clusters and water molecules hydrating these coding structures may act as complementary coding forms. According to some estimations, of all water in human organism, approximately 60% is free water, while 40% is involved with hydration of biological molecules. Other estimations give that only 5% of free water may be in cluster forms by the sphere packing law of coding number 12, while the rest 95% of free water is in form of "chaos" with local polymerized islands. So, we can state that, despite significant progress in science and our understanding of water, organization of water in living system is still a mystery.

According to the coding approach based on sphere packing, optimal water organization should be as a hydrogen-bonded $(H_2O)_n$ polyhedron $5^{12}6n$ ($n = 0, 2, 4\ldots$), where 5^{12} represents 12 pentagons and n different number of hexagons. Through hydrogen bonds dynamics, this water clathrate possesses spherical coding system $2^5 = 32$. Having in mind that arrangement of water, based on number 12, may represent a coding system, which is a part of optimal information peak (11, 12, and 13) of sphere packing, then water hydrogen-bonded polyhedron is both compatible and complementary coding system with the genetic code (DNA and proteins) (Koruga, 2012).

This knowledge has important implications. What is usually considered as "junk" sequence in the genetic code may actually perform an active regulatory role, through its influence on water molecular organization. And water thus serves as one more coding system within the human body. For the better understanding of the water role we include a new approach—Aquaphotomics (Tsenkova, 2010b).

4.2 Aquaphotomics of Nanoharmonized Substance

Aquaphotomics is a new expression recently introduced to describe the new scientific concept based on using water as a multielement system that could be well described by its multidimensional spectra (Tsenkova, 2010b). Aquaphotomics is a

method and a scientific discipline based on visible-near infrared spectroscopy (vis-NIRS) and multivariate spectral analysis. Visible infrared (vis-NIR) spectroscopy has proved to be a powerful tool and source of information and it facilitates the establishment of Aquaphotomics, for dynamic, noninvasive studies (Tsenkova, 2010b).

In order to understand the water molecular organization under the influence of nanoharmonized substance, the Aquaphotomics approach was used in studies of aqueous solutions of nanoharmonized substance, Nanocream—newly designed skin cream based on nanoharmonized substance, and consequently how this cream affect skin properties (Tsenkova, 2010b).

Aquaphotomics knowledge is based on years of research experience in vis-NIR spectroscopy of water and different aqueous and biological systems under various perturbations. Systematization of knowledge resulted in the identification of 12 characteristic wavelength ranges (6–20 nm width each) in the area of the first overtone of the water NIR spectra, where despite of the type of perturbation the observed systems showed predictable spectral variations. To visualize these changes of water absorbance pattern a star chart named "aquagram" is used (Tsenkova, 2010a); it displays normalized absorbance values at several water absorbance bands on the axis originating from the center of the graph. Water spectral pattern displayed on the aquagram can be considered as a "mirror on molecular level," reflecting functionality of the structures present in water (Tsenkova, 2010a,b).

Aquaphotomics has been successfully applied in various fields from water science, agriculture, to early diagnostics (Chatani et al., 2014; Goto et al., 2015; Gowen et al., 2009, 2011, 2013; Jinendra et al., 2010; Matija et al., 2015; Munćan et al., 2014; Sakudo et al., 2012; Tsenkova, 2007, 2008).

The aquagram (Fig. 4.11) shows the characteristic absorbances of analyzed aqueous systems in 12 characteristic wavelength ranges in the region of the first overtone of water in NIR region for undiluted nanoharmonized substance and pure water. From the aquagram, one can see the differences in hydrogen bonds network typical for pure water and in comparison for undiluted nanoharmonized substance. It is clear from the aquagram that undiluted nanoharmonized substance shows organization of water molecules in water clusters with 2, 3, and 4 hydrogen bonds (S_2, S_3, and S_4) and bonded water (1518 nm, ν_1, ν_2). Compared to pure water it is obvious that NHS acts as a structuring element in water making strong hydrogen bonds.

4.3 Analysis of Nanocream Effects on the Skin

The NIR spectral analysis and Aquaphotomics were applied to investigate the effect of the nanocream (cream based on nanoharmonized substance) on the skin. A preliminary study has been designed in order to observe effects on water in skin when the nanocream is applied.

The investigated nanomaterial nanoharmonized substance (NHS) is basically a hydrated hydroxylated fullerene, which has a harmonized form Φ/ϕ. The harmonized form of this substance whose composition follows Fibonacci sequence is a

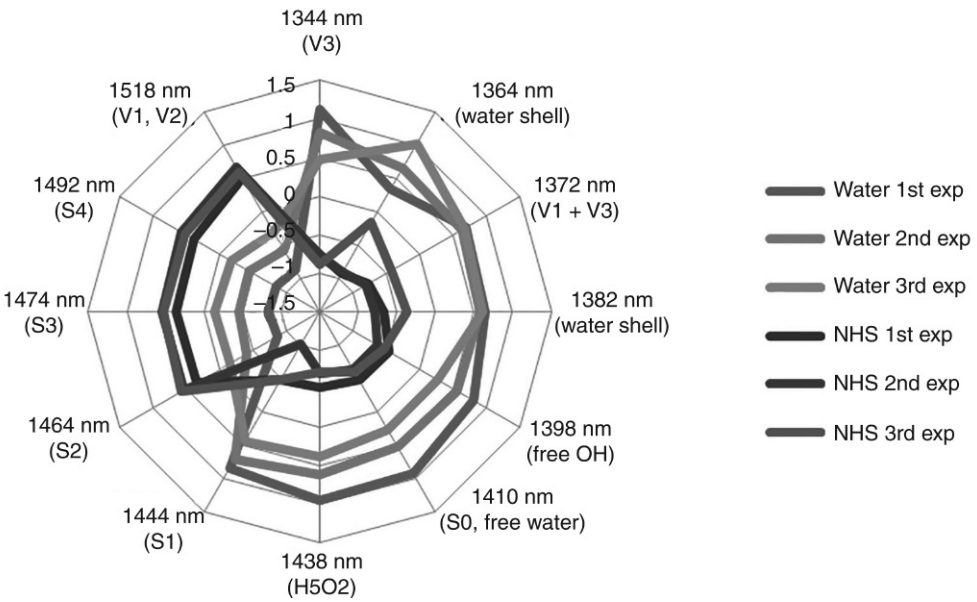

FIGURE 4.11 Aquagram. Compartment of water frequency state for 12 vibration modes (in range 1344–1518 nm) and undiluted nanoharmonized substance for same spectral window.

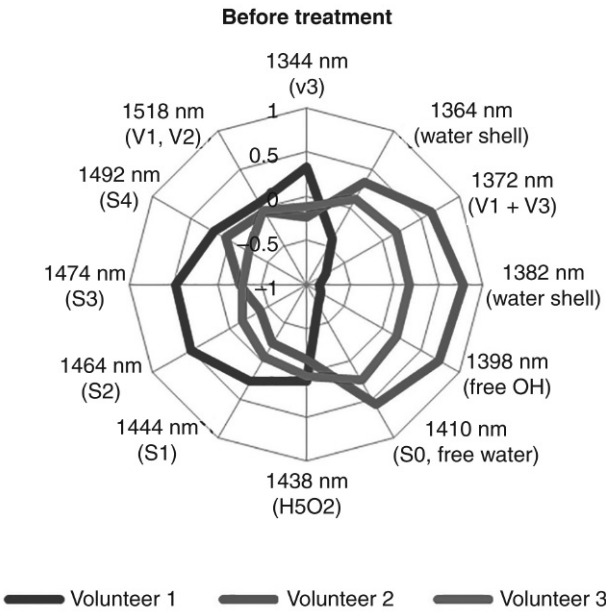

FIGURE 4.12 Comparison of skin condition for three volunteers (average for 3 days).

result of idea of creating nanocontrolling device, which can conduct harmonized vibrations to water molecules in near surroundings and force biomolecules to recover its natural vibration mode. The importance of harmonization of vibrations for restoring functions of otherwise damaged biomolecules is discussed in previous work (Matija et al., 2012). The NHS substance was added to conventional nonbioactive substance and the skin cream was formed. Nanocream was produced in Intercosmetica, Neuchatel, Switzerland.

The used samples were Millipore water (Milli Systems Co., USA) and nanoharmonized substance (NanoWorld AG, Serbia). Nanoharmonized substance is a mixture of 50 μg/L of $[C_{60}(OH)_{24}@72H_2O]^{\Phi/\phi}$ and 18.2 MΩ water (Millipore water) under influence of oscillatory magnetic field of 200 mT by the Fibonacci sequences in three cycles, for a total 27 min (Koruga, 2011).

The case study involved in vivo spectral recordings on three healthy female subjects of different ages (Volunteer 1, 23 years; Volunteer 2, 44 years; Volunteer 3, 25 years). The skin treatment consisted of daily application (3 times a day) of emulsion (solution of cream base) and nanocream (emulsion with added nanoharmonized substance) on two spots on the right arm, while left arm was left untreated to be used for comparison (control area). The whole treatment lasted for 8 days (Fig. 4.12).

Figs. 4.13–4.15 present aquagrams showing average skin condition for three different volunteers before any treatment. Normalized absorbance at respective water absorbance bands was calculated following the initial transformation of the NIR spectra of skin for each volunteer: (1) multiplicative scatter correction, (2) autoscaling for each wavelength, and (3) average spectra for 3 days. Major differences in skin condition between all volunteers was observed before any treatment. It is interesting to notice, that the skin of the oldest human subject (second volunteer), has pronouncedly more free, unbound, water (S0), free OH, more water molecules in water shells and more water molecules with combination of symmetrical stretching fundamental vibration and H_2O antisymmetrical stretching vibration (1372 nm, $\nu 1 + \nu 3$), while less water bound in dimers and trimmers, comparing to two young volunteers. The aquagrams of the skin for first, second, and third volunteer are presented in Figs. 4.13–4.15, respectively. Comparison of untreated and treated skin with emulsion and nanocream shows evident differences in each volunteer's skin after treatment. The common feature for all volunteers' aquagrams after treating skin with emulsion is lower absorbance at 1344 nm (water shell), 1372 nm (combination of $\nu 1 + \nu 3$), 1382 nm (water shell), 1398 nm (free OH), and 1410 nm (free water), and higher absorbance at 1444, 1464, 1474, and 1492 nm (water molecules making 1, 2, 3, and 4 hydrogen bonds) and 1518 nm (bound water). This suggests that during the penetration in skin, emulsion favors creating bonds between water molecules in skin. Application of the nanocream leads to: higher absorbance at 1344 nm (symmetric stretching), 1438 nm (H_2O–R, both lone pairs of the oxygen electrons bound to water clusters), 1444, 1464, and 1474 nm (water molecules making 1, 2, and 3 hydrogen bonds), whereas less absorbance is observed at 1372 nm (combination of $\nu 1 + \nu 3$), 1382 nm (water shell), 1398 nm (free OH), and 1410 nm (free water) similar to effect of emulsion only. It can be concluded that application of emulsion and nanocream in case of these three volunteers,

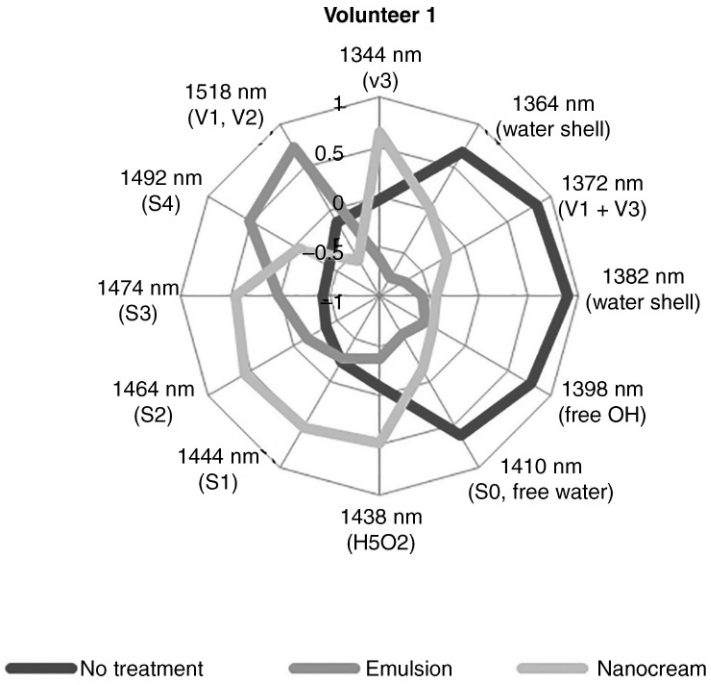

FIGURE 4.13 Aquagram of untreated and treated skin with emulsion and nanocream for Volunteer 1.

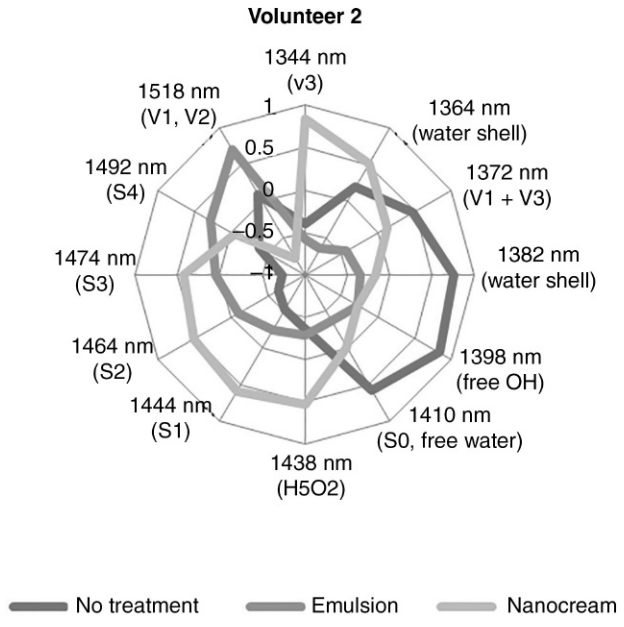

FIGURE 4.14 Aquagram of untreated and treated skin with emulsion and nanocream for Volunteer 2.

lead very quickly since its first application to reorganization of skin water from unbound state to mostly bounded, but in different ways. Nanocream, comparing to emulsion does not create larger water formations (1492 nm, water pentamers, and 1518 nm strongly bounded water).

4.4 Case Study of NHS Therapeutic Effects on Skin

In this case study human skin was treated everyday during 2 months. Twelve cross-sections of skin were analyzed on collagen, elastin, and capillaries. Four different evidences of fullerene influence on biological activities was observed: increasing numbers of cell growth in derma, increasing number of collagen and elastin fibers, and different status of capillaries of derma (Matija et al., 2004). The gold standard for definite diagnosis is histopathology and therefore biopsy from male skin was done before and after a 2-month treatment.

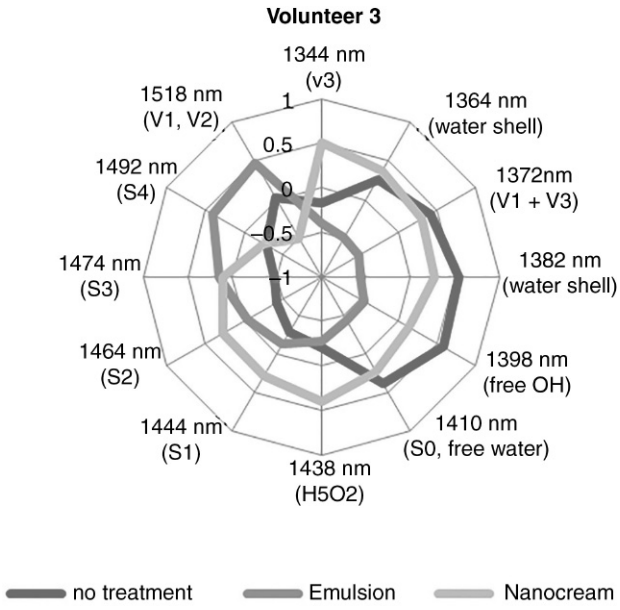

FIGURE 4.15 Aquagram of untreated and treated skin with emulsion and nanocream for Volunteer 3.

The procedure was as follows. Skin specimens were taken incisional by scalpel, biopsy preceded with local anesthesia by 2% lidocaine solution. The volume fixative was 20 times the volume of the specimen. After at least 72 h of fixation, the specimens were placed in 96% alcohol for 12 h following by their placing in 100% alcohol for 3–5 h. The specimens were placed in alcohol and then in a xylol solution and kept for 3 h. Tissue processing was followed by using paraffin wax for embedding process. Fixation was performed with lower melting temperature paraffin (52–54°C) for extraction of xylol, followed by embedding in higher temperature melting paraffin (58–60°C). After cooling, paraffin blocks containing tissue were cut on a microtome into 3–5 μm slices that were fixed to glass tiles in warm water. Each tile was dried overnight. After cooling, each specimen was stained with hematoxylin and eosin and with orcein for elastic fibers visualization. Microscopic examination was performed at 10 and 40 times magnification and digital images were taken (Matija et al., 2004).

The difference in derma before and after treatment is presented in Fig. 4.16. It was observed that not only a higher number of cells in derma exist, but the order of cells is present. Derma is richer in collagen and elastin fibers. Around capillaries in derma there are more tissue elements, which support their elasticity. Derma is richer with fibroblasts and eosinophils. The feedback control mechanism of these effects is still not completely elucidated, but we proposed one based on torsion pendulum as well as on intermolecular biophysical communication system. There are some special polypeptide chains that can be structurally compatible with fullerenol. The translation–rotation symmetry law gives torsion angles of C_{60} and $C_{60}(OH)_{24}$ some values, but values of the rotation angles (cp, and y_i) of peptide planes around C–C and N–C_{aj} are different. The best fitting of $C_{60}(OH)_{24}$ with protein is achieved on places where order of amino acids is Asp–Gly–Val (discovered in stereomyces subtilisin inhibitor) or Gly–Tyr (discovered in the structure T-cell, molecule Cd8A, chain H) (Friedman et al., 1993).

The $C_{60}(OH)_{24}$–amino acid (protein chain) interaction may happen in two different ways. The first one is based on London forces between peptide planes and $C_{60}(OH)_{24}$ having the same torsion angles. The second interaction is based on the torsion pendulum principal. The $C_{60}(OH)_{24}$ is a torsion pendulum body suspended from O---H bond (as a wire) with amino acid. When the body [$C_{60}(OH)_{24}$] is rotated at an angle θ from its equilibrium position, the bond is twisted, exerting a torque on the body (Fig. 4.17). The torque opposes the displacement θ and, if the twisting is not too large, has a magnitude proportional to θ as $T = -k\theta$ (k—the torsion coefficient of the bound). The period of oscillation of the body is $p = 2\pi(I/k)1/2$, where I is the momentum of inertia of the body around bond. Angular frequency is $\omega_o = (Id1)^{1/2}$, which can be coupled with the internal frequency of body.

Momentum of inertia of $C_{60}(OH)_{24}$ can be calculated (Matija et al., 2004) as:

$$I = \Sigma m_i r_i^2 = 60 m_c r_c^2 + 24 m_o r_o^2 + 24 m_H r_H^2$$
$$= \left(60 \times 12 \times 0.355^2 \cdot 10^{-18} + 24 \times 16 \times 0.425^2 \cdot 10^{-18} + 24 \times 1 \times 0.475^2 \cdot 10^{-18}\right) \cdot 1.67 \cdot 10^{-27} = 1.1056 \cdot 10^{-42}\,\text{kg/m}^2$$

where m_c, m_o, and m_H are a mass of carbon, oxygen, and hydrogen, respectively, r_c r_o and r_H are distance from the center of mass, while $C_{60}(OH)_{24}$ basic rotation in solution is 1.8×10^{10} s^{-1} that gives rotational energy value of fullerol

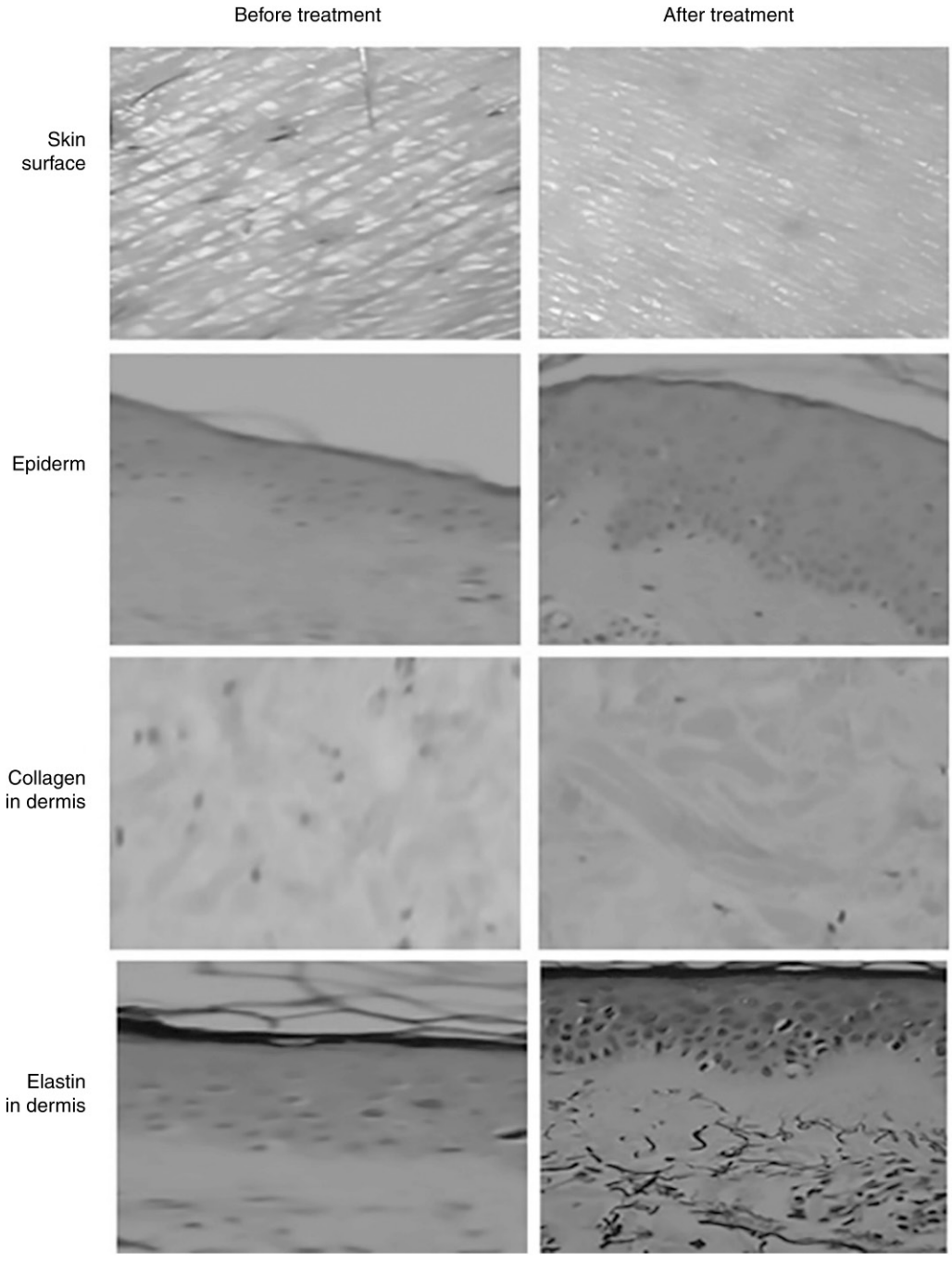

FIGURE 4.16 Experimental results of dermal, collagen, elastin, and capillaries status before and after human skin treatment by NHS. There is significant improvement of skin surface texture, thickness of epidermis, and presence of both collagen and elastin. Eight weeks of treatment led to advanced wrinkle reduction, smoother skin texture, greater vitality, and circulation. Epidermis is rejuvenated: there is significant increase in number of cells and 87% increase in thickness. Collagen growth is stimulated: there was 38%–85% increase in collagen with smoother organization of collagen fibers. Elastin growth is also noticeable with 40%–80% increase in number of elastin molecules with improved organization of elastin network.

3.3×10^{-22} J. This energy turns to be in resonance (coupling oscillation) with peptide plane through C═O vibration at 6 ± 0.05 μm wavelength, or 1660 ± 20 cm^{-1} wave number. Based on investigations in biology (Aslanidi et al., 2000) "nanotwister" can influence the soliton mechanism in alpha helix of collagen.

It is presented (Matija et al., 2004) that $C_{60}(OH)_{24}$—amino acid interaction, energy states of $C_{60}(OH)_{24}$ may be transmitted to peptide plane that influence conformation state of protein. In addition, it was reported (Koruga et al., 2004; Matija et al., 2004) that difference between the energies of two successive peptide planes is equal to the system entropy.

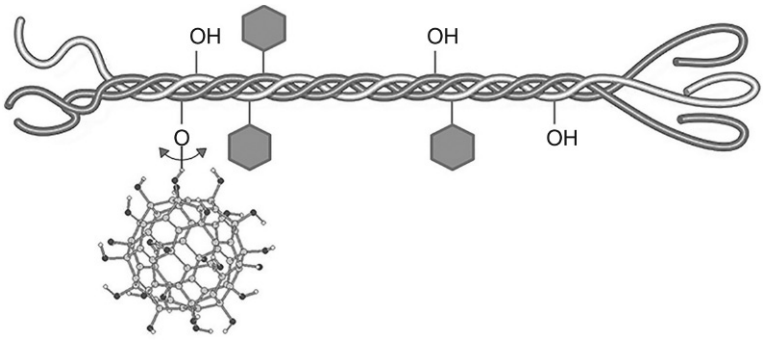

FIGURE 4.17 **Nanotwister.** Fibonacci nanostructure $C_{60}(OH)_{24}$ and collagen amino acid interaction (Matija et al., 2004).

Thanks to this biophysical mechanism, it is possible to make a feedback system for tissue regulation from extracellular matrix (collagen) through cell membrane (integrin) and cytoskeleton (actin and microtubules) to nucleus (Koruga et al., 1992; Matija, 2004; Rakočević, 1998). Also, it was demonstrated (Yin et al., 2013) that $C_{60}(OH)_{24}$ can influence the structure and assembly of collagen molecules and that $C_{60}(OH)_{24}$ interact with multiple polypeptide chains or with multiple collagen molecules, acting as a "fullerenol-mediated bridge" between the collagen peptides that enhance the interaction within or among collagen molecules. In addition, the interference of fullerenols on the interactions among collagen molecules may affect further the assembly of collagen fibrils, which results in the reduction of the mechanical stability of the collagen matrix (Yin et al., 2013).

Finding that continuous application of nanoharmonic preparations has led to the rejuvenation of the skin is of special interest, not only at clinical but also at histology level. It is well known that loss of functional elastic fibers and collagen lead to skin aging as well as exposure to the sun. For years, all-transretinoic acid has been used for the purpose of skin rejuvenation, but it results in side effects, such as skin dryness, peeling, erythema, and irritation (Craven and Griffiths, 2000). The NHS substance, presented here, has similar clinical and histological response, but to our knowledge, it does not cause the aforementioned side effects, which is a very good result compared to conventional traditionally used antiaging all-transretinoic acid.

4.5 Violation of the DNA-Protein-Water Information Channel and Cancer

Nowadays, numerous studies are dedicated to the knowledge improvement of cancer disease because it is one of leading causes of death in the last century. One of the approaches in the cancer mechanism understanding might be consideration of cancer as symmetry breaking phenomena of hydrogen bonds, based on the synergy of DNA-microtubule-water coding system based on hydrogen bonds (perfect numbers and Golden Mean).

Since we are considering here the influence of NHS to skin it is important to underline that the penetration of cancer from epidermis into dermis "opening the door" for methastasis and causing collagen distortion below the basal membrane (lamina fibroreticularis). On other hand it has to be taken into account that the epidermis represents a dynamic renewing structure, which provides life-sustaining protection from the environment, while keratinocytes and melanocytes are the major cell types of the epidermis (starting as stem cells in the basal epidermal layer). It is important to say that the cells stop to divide and go through morphological changes in order to create the spinous, granular, transition, and cornfield layers (Gawkrodger and Ardern-Jones, 2012) due to keratinocytes moving to the epidermal surface. It is well known that one melanocyte cell may overlap a few keratinocytes giving them melanin (the mechanism is yet unknown), which is responsible for protection from the environmental electromagnetic radiation (UV radiation) and neutralization of free radicals (Koruga, 2012; Varani et al., 2004).

In order to understand how metastases arise we need to clarify how collagen distortion below the basal membrane occurs. As normal collagen type I [$\alpha1(I)_2\alpha2(I)$] consists of two procollagen chains: $\alpha1(I)$, having gene located on chromosome 17 (q21–q22), and $\alpha2(I)$, having gene located on chromosome 7 (q21–q22), we can say that, from a classical communication channels point of view, it is the gene expression responsibility. Now, if we include quantum theory, we can also identify the quantum communication channel (entanglement) based on DNA hydrogen bonds, between keratinocyte or melanocyte and fibroblast cells. The key point is symmetry-breaking of hydrogen bonds in DNA, that through DNA-microtubule-water coding entanglement, initiates the breakdown (disconnection) of the classical and quantum communication synergy. In literature (Cornil et al., 1991), experimental evidence, which indicates that fibroblast cells and human melanoma cells interact as a function of tumor progression, is provided. In the case when DNA on chromosome 7 is damaged by UV radiation,

in keratinocyte or melanocyte cells, this information will be transferred to both centrioles (damaged cell) and fibroblast cells in regions through nonclassical quantum channels. This will lead to a dysfunction of centrioles, which will start to divide chromosomes irregularly and the initial cancer cell nucleus will become bigger than in a normal cell. The number of dysfunctional cells will increase rapidly due to a positive water-centriole feedback control mechanism that will change centriole pairs orthogonality (Koruga et al., 1992). Further, collagen α2(I) will not be produced by fibroblast cells, which in its absence, will incorporate one more α1(I) procollagen chain during assembly of procollagen chains into procollagen molecule. The result will be collagen type I-trimer having structure $[\alpha 1(I)_3]$. As links between procollagen chains do not fit well in I-trimer, collagen will lose OH groups and free water molecules will occur.

In tissue, increasing the free water volume up to 20% will be achieved, which is very similar during the skin aging, which is one of the reasons older people are more likely to suffer from cancer. The domination of the mentioned type of collagen the given tissue makes weak lamina fibro-reticular (as a "woof" of basal lamina), due to inadequate interconnection, based on hydrogen bonds, between procollagen chains into procollagen molecule.

4.6 Case Study of NHS Medical Therapy

Experiments were done in ORS Hospital, Belgrade, and involved eight volunteers, who signed approval for treatment. Here three cases are presented: basal cellular carcinoma syndrome (Fig. 4.18), and two scars (Figs. 4.19 and 4.20). Fig. 4.18 presents the difference in skin condition before and after 8 weeks of treatment. The patient is 83 years old, having basal cellular carcinoma, which was not operable. The skin cream was applied at areas denoted by the green arrows, while white arrows point to the nontreated area. After 8 weeks, the treated skin area showed improved skin condition, while the nontreated area deteriorated.

In Figs. 4.19 and 4.20, two patients, 58 years old, were treated after surgical intervention. After 8 weeks of treatment by cream, the scars are practically invisible without skin tension, and have a natural skin color.

5 CONCLUSIONS

Nanomedicine, both therapeutically and diagnostically, is a challenge for science, technology, and engineering. From a scientific point of view there are many phenomena, like fractal properties of matter, synergy structure-energy-information in biological systems, quantum control of DNA, and water-biomolecules interaction, which should be much better understood. We conserved and proposed some approaches of biomolecular signaling but there is a lot of room for new approaches that have not been considered, like quantum entanglement, quantum tunneling, and soliton phenomena.

In our approach we considered collagen-integrin-microtubule signaling based on oscillatory process of peptide planes in their chains. It is clearly shown (Fig. 4.7) that these three biomolecules interact resonantly and transmit signals from extracellular space to cytoplasm and cell nucleus smoothly.

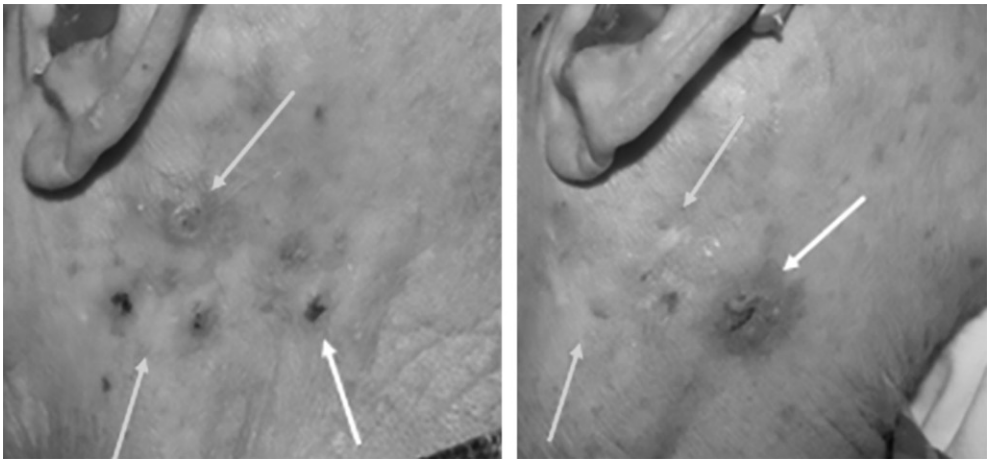

FIGURE 4.18 Example of therapeutic effects of Fibonacci nanostructures (NHS) on basal cellular carcinoma syndrome. Regions indicated by *green arrows* are treated by NHS, while region indicated by *white arrow* is not. After 8 months of treatment, the result is presented on figure left: regions that are treated by NHS look better, region that is not treated aggravate. Skin lesions treated with NHS regressed in total or partially. Patient observed that the itchiness, scabs, peelings, and pain disappeared from the regions treated with the NHS.

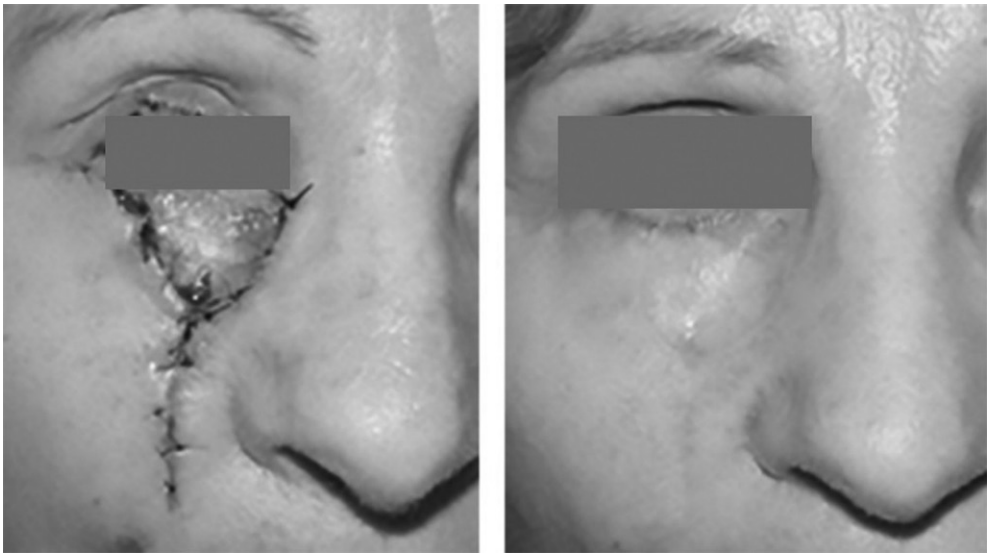

FIGURE 4.19 Example of therapeutic effects of Fibonacci nanostructures (NHS) on face scar. (Case 1): Image on the left presents the state of scar on the 7th day after surgery before removing the sutures. Image on the right presents the scar after 8 months of treatment using NHS. The scar is practically invisible, with no skin tension, almost natural skin color with slight hypopigmentation. Personal opinion of the patient is that treatment also led to the removal of the ectropion of the lower eyelid.

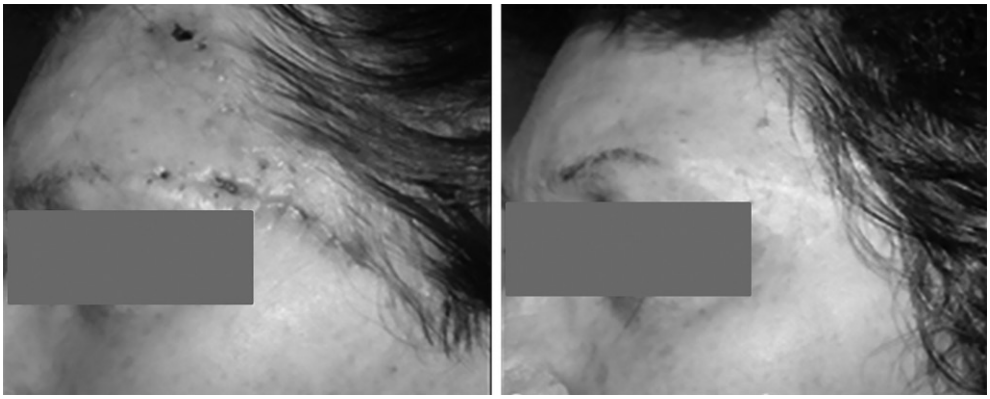

FIGURE 4.20 Example of therapeutic effects of Fibonacci nanostructures (NHS) on face scar. (Case 2): Image on the left is the state of scar 14 days after excision. Image on the left presents state of scar after 3 months of NHS treatment.

The results of this preliminary investigation on the effects of skin cream, which contains fullerene-based nanomaterials with a harmonized form Φ/ϕ, lead to the conclusion that it produced considerable difference in skin condition very soon after application. The apparent change after application on the skin is a consequence of skin–water reorganization and formation of additional hydrogen bonded water molecules. Taking into account the results of biopsy, histological images and scar tissues after cream application it could be concluded that this is more favorable state of organization of water. Whether this state of water in tissues is organizing influence or a consequence it cannot be said at this point. These results are only preliminary, obtained for limited number of cases and further investigation is needed in order to gain statistically significant result. The integrin, as linking biomolecule between extracellular space and cytoplasm, is a family of receptors that forms a diverse group of molecules, which through their interactions with different matrix molecules and with different cytoskeletal elements can generate a wide range of cellular responses. It is now evident that integrin mediated signaling can influence proliferation, apoptosis, differentiation, and migration, and their involvement in such fundamental processes suggests that altered function or expression of integrins by a cell may influence the development of the malignant phenotype (Jones and Walker, 1999). However, more research has to be done for fully understanding the signaling process between extracellular space and cell nucleus (DNA).

Fibonacci nanostructures as DNA, clathrin, microtubules exist in biological systems. However, any type of protein and enzymes energetically follow the Golden Mean law.

The last decade in science has seen significant discoveries: evidences of multiple structures based on Fibonacci numbers in numerical patterns in DNA (Perez, 2015) and the importance of waves and water in the process of propagation of the information contained in the DNA (Montagnier et al., 2011). The possibility that DNA is not just matter, in other words classical system, but also quantum has been neglected. The same applies for the importance of water in biological organisms. Many of these phenomena are still not understood well, and it will probably take a long time to reach full understanding. However, even if we don't understand still how nature works, we believe that the good solution for the future therapy and nanomedicine is to mimic nature's solutions.

ACKNOWLEDGMENTS

The completion of this research would not be possible without Ministry of Education and Science of the Republic of Serbia who partially funded it through projects from 1995 to 2000 and 2008 to 2015 (Project III-41006) and Zepter International from 2002 to 2005. In particular, the authors would also like to express their deep appreciation to MD Jadran Bandic and ORS Hospital, Belgrade for his help, as well as to Mr. Yutaro Tsuchisaka, MSc, researcher in the Biomeasurement Laboratory, Kobe and Professor Roumiana Tsenkova, Kobe University, Japan where part of the experiments was conducted.

REFERENCES

Andrievsky, G.V., Bruskov, V.I., Tykhomyrov, A.A., Gudkov, S.V., 2009. Peculiarities of the antioxidant and radioprotective effects of hydrated C 60 fullerene nanostuctures in vitro and in vivo. Free Rad. Biol. Med. 47, 786–793.

Aslanidi, K., Pogorelov, A., Aslanidi, V., Mornev, A., Sahakyan, G., 2000. Potassium gradients in the growing hyphae of neurospora crassa. Memb. Cell Biol. 14, 487–495.

Bao, H., Pan, Y., Ping, Y., Sahoo, N.G., Wu, T., Li, L., Li, J., Gan, L.H., 2011. Chitosan-functionalized graphene oxide as a nanocarrier for drug and gene delivery. Small 7, 1569–1578.

Bernstein, L.J., 1992. Energy localisation and non-linear dimmer. Nanobiology 1, 251–269.

Blundell, T.L., Johnson, L.N., 1976. Protein Crystallography. Academic Press, New York, NY.

Cha, C., Shin, S.R., Annabi, N., Dokmeci, M.R., Khademhosseini, A., 2013. Carbon-based nanomaterials: multifunctional materials for biomedical engineering. ACS Nano 7, 2891–2897.

Chai, B., Pollack, G.H., 2010. Solute-free interfacial zones in polar liquids. J. Phys. Chem. B 114, 5371–5375.

Chatani, E., Tsuchisaka, Y., Masuda, Y., Tsenkova, R., 2014. Water molecular system dynamics associated with amyloidogenic nucleation as revealed by real time near infrared spectroscopy and aquaphotomics. PLoS One 9, e101997.

Chen, Z., Meng, H., Xing, G., Chen, C., Zhao, Y., Jia, G., Wang, T., Yuan, H., Ye, C., Zhao, F., 2006. Acute toxicological effects of copper nanoparticles in vivo. Toxicol. Lett. 163, 109–120.

Cornil, I., Theodorescu, D., Man, S., Herlyn, M., Jambrosic, J., Kerbel, R., 1991. Fibroblast cell interactions with human melanoma cells affect tumor cell growth as a function of tumor progression. Proc. Natl. Acad. Sci. 88, 6028–6032.

Craven, N., Griffiths, C., 2000. Photoageing. Springer, New York, NY.

Curie, P., 1894. Sur la symetrie dans les phenomenes physique. Symetrie d'un champ electrique et d'un champ magnetique. J. Phys. 3, 393–417.

Donaldson, K., Aitken, R., Tran, L., Stone, V., Duffin, R., Forrest, G., Alexander, A., 2006. Carbon nanotubes: a review of their properties in relation to pulmonary toxicology and workplace safety. Toxicol. Sci. 92, 5–22.

Feng, L., Liu, Z., 2011. Graphene in biomedicine: opportunities and challenges. Nanomedicine 6, 317–324.

Friedman, S.H., DeCamp, D.L., Sijbesma, R.P., Srdanov, G., Wudl, F., Kenyon, G.L., 1993. Inhibition of the HIV-1 protease by fullerene derivatives: model building studies and experimental verification. J. Am. Chem. Soc. 115, 6506–6509.

Gawkrodger, D., Ardern-Jones, M.R., 2012. Dermatology: An Illustrated Colour Text, fifth Revised ed. Elsevier Health Sciences, Churchill Livingstone, London.

Ge, C., Du, J., Zhao, L., Wang, L., Liu, Y., Li, D., Yang, Y., Zhou, R., Zhao, Y., Chai, Z., 2011. Binding of blood proteins to carbon nanotubes reduces cytotoxicity. Proc. Natl. Acad. Sci. 108, 16968–16973.

Geim, A.K., 2009. Graphene: status and prospects. Science 324, 1530–1534.

Gharbi, N., Pressac, M., Hadchouel, M., Szwarc, H., Wilson, S.R., Moussa, F., 2005. [60]Fullerene is a powerful antioxidant in vivo with no acute or subacute toxicity. Nano Lett. 5, 2578–2585.

Gilbert, N., 2009. Nanoparticle safety in doubt. Nat. News 460, 937.

Goto, N., Bazar, G., Kovacs, Z., Kunisada, M., Morita, H., Kizaki, S., Sugiyama, H., Tsenkova, R., Nishigori, C., 2015. Detection of UV-induced cyclobutane pyrimidine dimers by near-infrared spectroscopy and aquaphotomics. Sci. Rep. 5, 1–13.

Gowen, A., Amigo, J., Tsenkova, R., 2013. Characterisation of hydrogen bond perturbations in aqueous systems using aquaphotomics and multivariate curve resolution-alternating least squares. Anal. Chim. Acta 759, 8–20.

Gowen, A.A., Tsenkova, R., Esquerre, C., Downey, G., O'Donnell, C.P., 2009. Use of near infrared hyperspectral imaging to identify water matrix coordinates in mushrooms (agaricus bisporus) subjected to mechanical vibration. J. Near Infrared Spectrosc. 17, 363.

Gowen, A.A., Tsuchisaka, Y., O'Donnell, C., Tsenkova, R., 2011. Investigation of the potential of near infrared spectroscopy for the detection and quantification of pesticides in aqueous solution. Am. J. Anal. Chem. 2, 53.

Hynes, R.O., 2002. Integrins: bidirectional, allosteric signaling machines. Cell 110, 673–687.

Iijima, S., 1991. Helical microtubules of graphitic carbon. Nature 354, 56–58.
Isaacs, E., Shukla, A., Platzman, P., Hamann, D., Barbiellini, B., Tulk, C., 1999. Covalency of the hydrogen bond in ice: a direct X-ray measurement. Phys. Rev. Lett. 82, 600.
Jeffrey, G., 1997. An Introduction to Hydrogen Bonding. Oxford University Press, Oxford.
Jinendra, B., Tamaki, K., Kuroki, S., Vassileva, M., Yoshida, S., Tsenkova, R., 2010. Near infrared spectroscopy and aquaphotomics: novel approach for rapid in vivo diagnosis of virus infected soybean. Biochem. Biophys. Res. Commun. 397, 685–690.
Jones, J., Walker, R., 1999. Integrins: a role as cell signalling molecules. Mol. Pathol. 52, 208.
Juliano, R., Haskill, S., 1993. Signal transduction from the extracellular matrix. J. Cell Biol. 120, 577.
Kang, S.-G., Huynh, T., Zhou, R., 2012a. Non-destructive inhibition of metallofullerenol Gd@ C82 (OH) 22 on WW domain: implication on signal transduction pathway. Sci. Rep. 2, 1–7.
Kang, S.-G., Zhou, G., Yang, P., Liu, Y., Sun, B., Huynh, T., Meng, H., Zhao, L., Xing, G., Chen, C., 2012b. Molecular mechanism of pancreatic tumor metastasis inhibition by Gd@ C82 (OH) 22 and its implication for de novo design of nanomedicine. Proc. Natl. Acad. Sci. 109, 15431–15436.
Koruga, D., 1993. Fullerene C60: History, Physics, Nanobiology, Nanotechnology. Elsevier Science Ltd., New York, NY.
Koruga, D., 1997. Holopent and information physics. Brain and Consciousness, p. 179.
Koruga, D., 2011. Golden mean harmonized water and aqueous solutions. Google Patents.
Koruga, D., 2012. Classical and quantum information processing in DNA-protein coding. Springer, New York, NY.
Koruga, D., Andjelkovic, M., Jankovic, S., Hameroff, S., 1992. Cytoskeleton as feedback control system in neuron. Artif. Neural Netw. 2, 399–402.
Koruga, D., Tomić, A., Ratkaj, Ž., Matija, L., 2004. Gibbson: peptide plane as a unique biological nanostructure. Mater. Sci. Forum 453-454, 529–536.
Kroto, H.W., Heath, J.R., O'Brien, S.C., Curl, R.F., Smalley, R.E., 1985. C60: buckminsterfullerene. Nature 318, 162–163.
Kuhn, H., Forsterling, H., 2000. Principles of Physical Chemistry. John Wiley & Sons, Chichester.
Lanone, S., Andujar, P., Kermanizadeh, A., Boczkowski, J., 2013. Determinants of carbon nanotube toxicity. Adv. Drug Deliv. Rev. 65, 2063–2069.
Lee, J.S., Joung, H.-A., Kim, M.-G., Park, C.B., 2012. Graphene-based chemiluminescence resonance energy transfer for homogeneous immunoassay. ACS Nano 6, 2978–2983.
Li, M., Yang, X., Ren, J., Qu, K., Qu, X., 2012. Using graphene oxide high near-infrared absorbance for photothermal treatment of Alzheimer's disease. Adv. Mater. 24, 1722–1728.
Matija, L., 2004. Reviewing paper: nanotechnology: artificial versus natural self-assembly. FME Trans. 32, 1–14.
Matija, L., Koruga, D. (Eds.), 2007. Value of action as a criteria for classicala an quantum object consideration on molecular level. Serbian Society of Mechanics, Belgrade.
Matija, L., Koruga, D., Jovanović, J., Dobrosavljević, D., Ignjatović, N., 2004. In vitro and in vivo investigation of collagen-C60 (OH) 24 interaction. Mater. Sci. Forum 453-454, 561–566.
Matija, L., Muncan, J., Tsenkova, R., Mileusnic, I., Koruga, D., 2015. Aquaphotomic study of hydrated hydroxylated fullerene based on skin nanocream: water based nanomedicine. ITNANO2015, p. 17.
Matija, L.R., Tsenkova, R.N., Miyazaki, M., Banba, K., Muncan, J.S., 2012. Aquagrams: water spectral pattern as characterization of hydrogenated nanomaterial. FME Trans. 40, 51–56.
Matija, L., Tsenkova, R., Munćan, J., Miyazaki, M., Banba, K., Tomić, M., Jeftić, B., 2013. Fullerene based nanomaterials for biomedical applications: engineering, functionalization and characterization. Adv. Mater. Res. 633, 224–238.
Mattick, J.S., 2003. Challenging the dogma: the hidden layer of non-protein-coding RNAs in complex organisms. Bioessays 25, 930–939.
Montagnier, L., Aissa, J., Del Giudice, E., Lavallee, C., Tedeschi, A., Vitiello, G., 2011. DNA waves and water. J. Phys. 306, 012007.
Munćan, J.S., Matija, L., Simić-Krstić, J.B., Nijemčević, S.S., Koruga, Đ.L., 2014. Discrimination of mineral waters using near infrared spectroscopy and aquaphotomics. Hemijska Industrija 68, 257–264.
Nel, A.E., Mädler, L., Velegol, D., Xia, T., Hoek, E.M., Somasundaran, P., Klaessig, F., Castranova, V., Thompson, M., 2009. Understanding biophysicochemical interactions at the nano–bio interface. Nat. Mater. 8, 543–557.
Nel, A., Xia, T., Mädler, L., Li, N., 2006. Toxic potential of materials at the nanolevel. Science 311, 622–627.
Ngan, C.L., Basri, M., Tripathy, M., Karjiban, R.A., Abdul-Malek, E., 2015. Skin intervention of fullerene-integrated nanoemulsion in structural and collagen regeneration against skin aging. Eur. J. Pharm. Sci. 70, 22–28.
Nielsen, G.D., Roursgaard, M., Jensen, K.A., Poulsen, S.S., Larsen, S.T., 2008. In vivo biology and toxicology of fullerenes and their derivatives. Basic Clin. Pharmacol. Toxicol. 103, 197–208.
Novoselov, K.S., Geim, A.K., Morozov, S., Jiang, D., Zhang, Y., Dubonos, S.A, Grigorieva, I., Firsov, A., 2004. Electric field effect in atomically thin carbon films. Science 306, 666–669.
Perez, J.-C., 2013. The "3 genomic numbers" discovery: how our genome single-stranded DNA sequence is "self-designed" as a numerical whole. Appl. Math. 4, 37–53.
Perez, J., 2015. Deciphering hidden DNA meta-codes: the great unification & master code of biology. J. Glycomics Lipidomics 5, 2.
Plow, E.F., Haas, T.A., Zhang, L., Loftus, J., Smith, J.W., 2000. Ligand binding to integrins. J. Biol. Chem. 275, 21785–21788.
Rakočević, M.M., 1998. The genetic code as a golden mean determined system. Biosystems 46, 283–291.
Sakudo, A., Suganuma, Y., Sakima, R., Ikuta, K., 2012. Diagnosis of HIV-1 infection by near-infrared spectroscopy: analysis using molecular clones of various HIV-1 subtypes. Clin. Chim. Acta 413, 467–472.
Samsonovich, A., Scott, A., Hameroff, S., 1991. Acousto-conformational transitions in cytoskeletal microtubules—implications for neuro-like protein array devices. In: Abstracts of Papers of the American Chemical Society. American Chemical Society, Washington, DC.

Sanchez, V.C., Jachak, A., Hurt, R.H., Kane, A.B., 2011. Biological interactions of graphene-family nanomaterials: an interdisciplinary review. Chem. Res. Toxicol. 25, 15–34.

Schwartz, M.A., Schaller, M.D., Ginsberg, M.H., 1995. Integrins: emerging paradigms of signal transduction. Annu. Rev. Cell Dev. Biol. 11, 549–599.

Service, R., 2000. Is nanotechnology dangerous? Science 290, 1526.

Srichai, M.B., Zent, R., 2010. Integrin structure and function. Springer, New York, NY.

Tsenkova, R., 2007. Aquaphotomics: water absorbance pattern as a biological marker for disease diagnosis and disease understanding. NIR News 18, 14–16.

Tsenkova, R., 2008. Aquaphotomics: acquiring spectra of various biological fluids of the same organism reveals the importance of water matrix absorbance coordinates and the aquaphotome for understanding biological phenomena. NIR News 19, 13–15.

Tsenkova, R., 2010a. Aquaphotomics: water in the biological and aqueous world scrutinized with invisible light. Spectrosc. Eur. 22, 6–10.

Tsenkova, R., 2010b. Introduction: aquaphotomics: dynamic spectroscopy of aqueous and biological systems describes peculiarities of water. J. Near Infrared Spectrosc. 17, 303–313.

Varani, J., Schuger, L., Dame, M.K., Leonard, C., Fligiel, S.E., Kang, S., Fisher, G.J., Voorhees, J.J., 2004. Reduced fibroblast interaction with intact collagen as a mechanism for depressed collagen synthesis in photodamaged skin. J. Invest. Dermatol. 122, 1471–1479.

Wang, I.C., Tai, L.A., Lee, D.D., Kanakamma, P., Shen, C.K.-F., Luh, T.-Y., Cheng, C.H., Hwang, K.C., 1999. C60 and water-soluble fullerene derivatives as antioxidants against radical-initiated lipid peroxidation. J. Med. Chem. 42, 4614–4620.

Wang, X., Yang, L., Chen, Z.G., Shin, D.M., 2008. Application of nanotechnology in cancer therapy and imaging. CA Cancer J. Clin. 58, 97–110.

Yang, Z., Kang, S.-G., Zhou, R., 2014. Nanomedicine: de novo design of nanodrugs. Nanoscale 6, 663–677.

Yang, K., Wan, J., Zhang, S., Tian, B., Zhang, Y., Liu, Z., 2012. The influence of surface chemistry and size of nanoscale graphene oxide on photothermal therapy of cancer using ultra-low laser power. Biomaterials 33, 2206–2214.

Yin, S., Wu, Y.L., Hu, B., Wang, Y., Cai, P., Tan, C.K., Qi, D., Zheng, L., Leow, W.R., Tan, N.S., 2014. Three-dimensional graphene composite macroscopic structures for capture of cancer cells. Adv. Mater. Interfaces 1, 1300043.

Yin, X., Zhao, L., Kang, S.G., Pan, J., Song, Y., Zhang, M., Xing, G., Wang, F., Li, J., Zhou, R., Zhao, Y., 2013. Impacts of fullerene derivatives on regulating the structure and assembly of collagen molecules. Nanoscale 5, 7341–7348.

Zhang, Y., Ali, S.F., Dervishi, E., Xu, Y., Li, Z., Casciano, D., Biris, A.S., 2010. Cytotoxicity effects of graphene and single-wall carbon nanotubes in neural phaeochromocytoma-derived pc12 cells. ACS Nano 4, 3181–3186.

Zhang, Y., Petibone, D., Xu, Y., Mahmood, M., Karmakar, A., Casciano, D., Ali, S., Biris, A.S., 2014. Toxicity and efficacy of carbon nanotubes and graphene: the utility of carbon-based nanoparticles in nanomedicine. Drug Metabol. Rev. 46, 232–246.

Zhao, Y., Xing, G., Chai, Z., 2008. Nanotoxicology: are carbon nanotubes safe? Nat. Nanotechnol. 3, 191–192.

Zheng, J.-M., Chin, W.-C., Khijniak, E., Pollack, G.H., 2006. Surfaces and interfacial water: evidence that hydrophilic surfaces have long-range impact. Adv. Colloid Interface Sci. 127, 19–27.

Zuo, G., Kang, S.g., Xiu, P., Zhao, Y., Zhou, R., 2013. Interactions between proteins and carbon-based nanoparticles: exploring the origin of nanotoxicity at the molecular level. Small 9, 1546–1556.